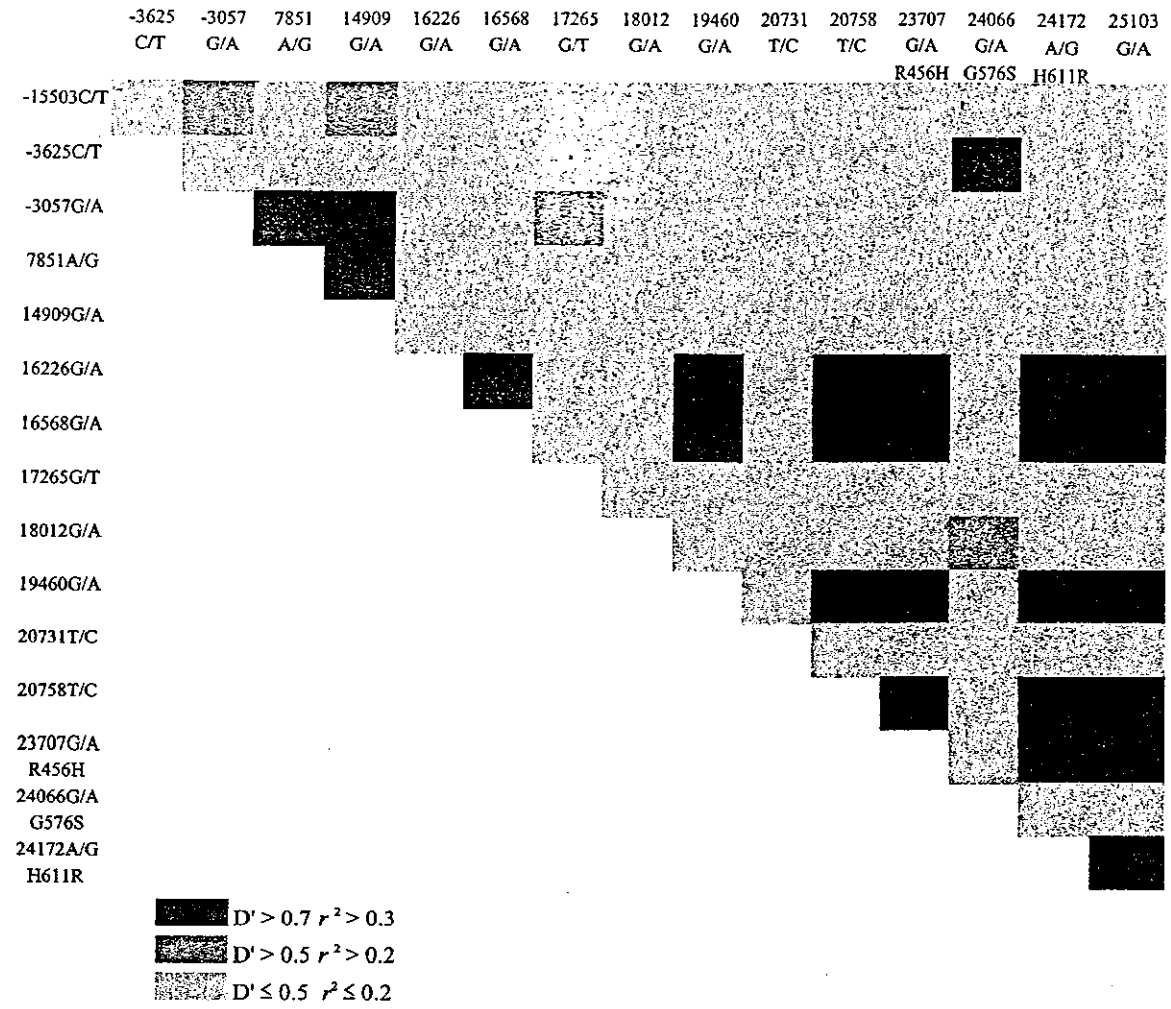

Fig. 2. Pairwise linkage disequilibrium in *WFS1* evaluated by D' and r^2. Extent of pairwise LD of *WFS1*, measured by two distinct coefficients, D' and r^2. Pairwise combinations are classified into three categories based on the degree of the observed LD. Pairwise combination with LD of $D' > 0.7$ and $r^2 > 0.3$, $D' > 0.5$ and $r^2 > 0.2$, and $D' \leqslant 0.5$ and $r^2 \leqslant 0.2$ is shown with black, dark grey, and grey box, respectively. The nucleotide indicates the location of the SNP relative to the A of the ATG of the initiator Met of *WFS1* (GenBank No. NT_006051).

and the others in exon 8. Of the cSNPs identified in this study, two (c. 402G>A, A134A; c. 1508T>G, V503G) were novel and not registered in the NCBI dbSNP database. None of the cSNPs were associated with bipolar disorder, but a novel cSNP (V503G) including four reported cSNPs (V395V, N500N, K811K, and S855S) was observed only in patients with bipolar disorder in a heterozygous state. Pairwise haplotype analysis was performed with combinations of eleven SNPs based on LD pattern (Fig. 3). The haplotype comprising g. −15503C/T and g. 16226G/A is most associated with bipolar disorder ($p = 0.006$), but does not reach significance after multiple adjustment Fig. 3. Association study with an increased number of samples is required.

Discussion

While Wolfram syndrome is rare, obligate carriers show increased prevalence of type 2 diabetes mellitus [9,10], and heterozygous carriers are reported to be 26-fold more likely to require hospitalization for psychiatric illness [11]. A relationship between psychiatric disorder and diabetes mellitus is suggested by mutations in *WFS1* that are observed in both diabetic and psychiatric phenotypes.

We estimated the LOD score for susceptibility to type 2 diabetes in one of the Wolfram pedigrees available and obtained suggestive maximum scores 1.20 and 2.67 at $\theta = 0$ for the dominant and the nonparametric model, respectively (unpublished), leading us to examine all exons of *WFS1* in type 2 diabetes. Ten cSNPs (A6T, Q14R, N159N, T170T, R228R, E237K, R383C, V412L, V412A, and D866N) were found only in patients with type 2 diabetes and not in those with bipolar disorder. Of these, seven cSNPs (A6T, A134A, N159N, T170T, E237K, R383C, and V412L) have not been reported previously [21]. This study shows that the minor alleles H456 and R611 are present more frequently in type 2 diabetic patients than in control subjects, while the

Table 2
Frequencies of coding SNPs in *WFS1* in patients with type 2 diabetes and controls

SNP	Amino acid change	Frequencies of minor allele		*P* value
		Patients ($n = 384$)	Controls ($n = 384$)	
g. 16 G>A	A6T*	0.0027	—	0.49
g. 41 A>G	Q14R*	0.0027	0.0026	>0.99
g. 11618 G>A	A134A*	0.019	0.0086	0.34
g. 13758 C>T	N159N*	0.0027	—	0.49
g. 13791 C>G	T170T*	0.013	0.0079	0.50
g. 14514 G>C	R228R	0.019	0.010	0.38
g. 14539 G>A	E237K*	0.0053	—	0.25
g. 23487 C>T	R383C*	0.0027	—	0.49
g. 23525 T>C	V395V	0.0054	0.0079	>0.99
g. 23574 G>C	V412L*	0.0081	0.0026	0.37
g. 23575 T>C	V412A	0.0054	0.0026	0.62
g. 23707 G>A	R456H	0.12	0.080	0.091
g. 23840 T>C	N500N	0.017	0.0079	0.33
g. 24066 G>A	G576S	0.087	0.11	>0.99
g. 24172 A>G	H611R	0.15	0.10	0.050
g. 24498 A>G	I720V	0.063	0.060	0.87
g. 24549 G>A	E737K	0.049	0.065	0.35
g. 24773 A>G	K811K	0.020	0.0079	0.21
g. 24809 C>T	I823I	0.0085	0.0026	0.73
g. 24905 G>A	S855S	0.017	0.0026	0.53
g. 24936 G>A	D866N	0.011	0.0052	0.44

The nucleotide indicates the location of the SNP relative to the A of the ATG of the initiator Met of *WFS1* (GenBank No. NT_006051). Asterisk indicates a novel polymorphism.

Table 3
Frequencies of haplotypes comprising R456H and H611R in patients with type 2 diabetes and controls

Haplotype	DM	Controls	χ^2	*P* value
R–H	0.83	0.89	6.206	0.013
R–R	0.04	0.03	1.334	0.248
H–H	0.01	0.00	—	0.069
H–R	0.12	0.08	2.207	0.137
	—	—	8.658	0.034

R–H in haplotype column is R456–H611 haplotype.

Table 4
Frequencies of coding-SNPs of *WFS1* in patients with bipolar disorder and in controls

Position genome	Position cDNA	Nucleotide change	Amino acid change	Exon	Frequencies of rare allele		*P* value
					Patients ($n = 94$)	Controls ($n = 192$)	
11618	402	G>A	A134A*	4	0.01	0.01	>0.999
23525	1185	T>C	V395V	8	0.01	0.00	0.33
23707	1367	G>A	R456H	8	0.07	0.08	0.91
23840	1500	T>C	N500N	8	0.01	0.00	0.33
23848	1508	T>G	V503G*	8	0.01	0.00	0.33
24066	1726	G>A	G576S	8	0.13	0.12	0.85
24172	1832	A>G	H611R	8	0.04	0.09	0.16
24498	2158	A>G	I720V	8	0.03	0.06	0.40
24549	2209	G>A	E737K	8	0.03	0.05	0.76
24773	2433	A>G	K811K	8	0.01	0.00	0.33
24809	2469	C>T	I823I	8	0.01	0.01	0.55
24905	2565	G>A	S855S	8	0.01	0.00	0.33

The nucleotide indicates the location of the SNP relative to the A of the ATG of the initiator Met of *WFS1* (GenBank No. NT_006051 for genome, AF 084481 for cDNA); asterisk indicates a novel polymorphism.

R456–H611 haplotype is significantly less frequent and the H456–R611 is more frequent in patients with type 2 diabetes. In the previous study, 370 Japanese patients with type 1 diabetes and 760 control subjects were analyzed, and H456 and R611 were found more frequently in patients than in controls. Preliminary studies in

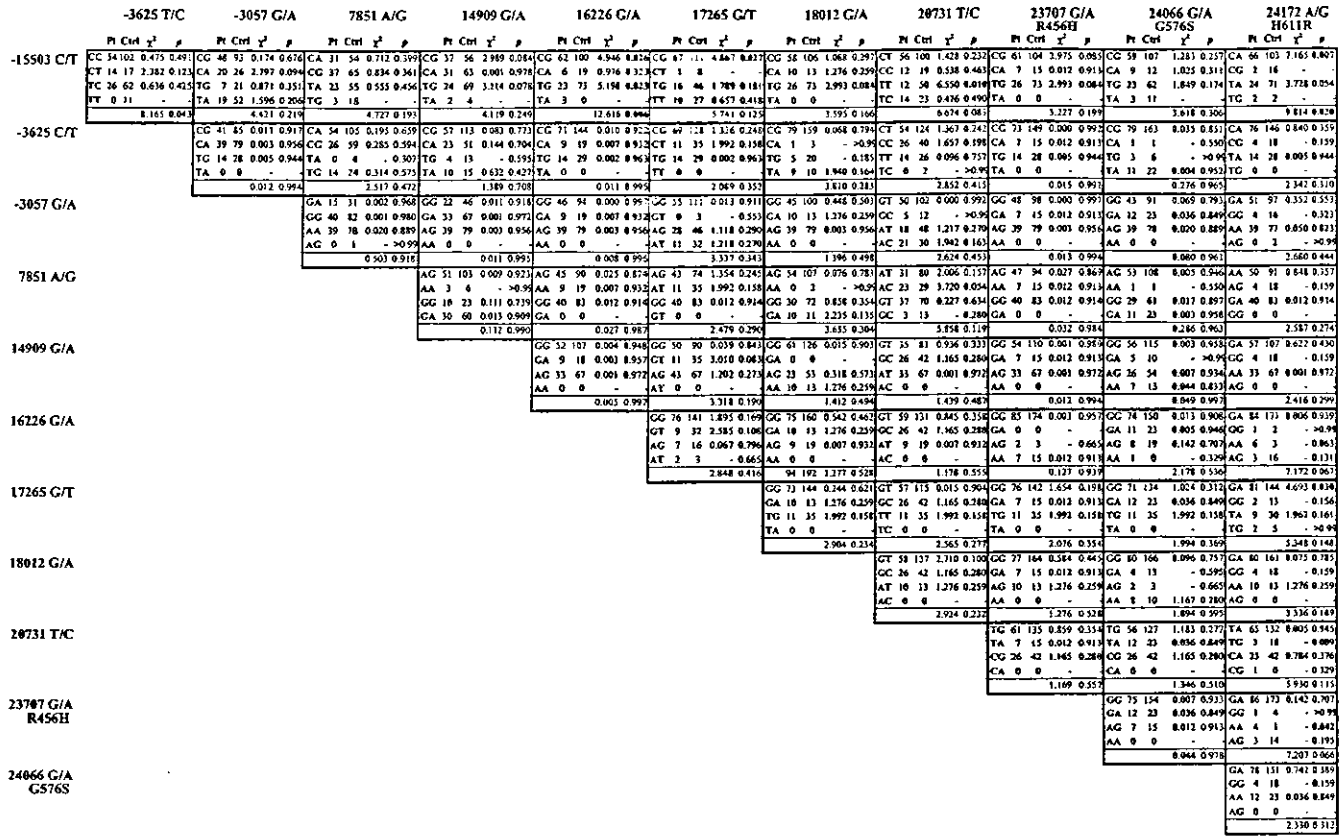

Fig. 3. Association study using pairwise haplotype frequencies in patients with bipolar disorder versus controls. In each cell, *P* values in the first through fourth row are based on 2×2 χ^2 test, and the *P* value in the last row is based on 2×4 χ^2 test. *P* value < 0.05 is indicated in bold.

patients with type 2 diabetes by the same group also showed a significant increase in H456 in type 2 diabetic patients compared to control subjects [22]. These results suggest the protective role of the H456, R611 and their haplotype in the pathogenesis of diabetes. However, the R456–H611 haplotype was found more frequently in type 2 diabetes in the UK [23], suggesting the presence of genetic heterogeneity among populations.

WFS1 is also a candidate for genetic predisposition to bipolar disorder because of the psychiatric phenotypes observed in both carriers and patients with Wolfram syndrome [2]. In addition, *WFS1* is located in a region that has been linked to bipolar disorder [12–14]. Ohtsuki et al. [24] examined exon 8 of *WFS1*, and found no association with bipolar disorder in Japanese. Kato et al. [25] examined four cSNPs (A559T, G576S, A602V, and H611R), and found no association with the disease in Japanese. In this study, we first performed mutation screening of all exons of *WFS1* in 47 Japanese patients with bipolar disorders, and identified 12 coding SNPs (Table 4). Two (c. 402G>A, A134A; c. 1508T>G, V503G) of these were novel, but none were significantly associated with bipolar disorder. To detect all of the polymorphisms in the *WFS1* gene, we examined about 50,000 bp covering the entire region of the gene in 12 Japanese subjects, and identified a total of 42 genetic variations. 18 SNPs and two insertion/deletion polymorphisms were identified in non-coding regions, and 22 SNPs were identified in coding regions. Pairwise haplotype analysis then was performed with combinations of eleven SNPs based on the LD pattern estimated using the 16 frequent SNPs (Fig. 2).

As shown in Fig. 3, we defined haplotypes by all possible pairs of 11 SNPs, and examined the associations with bipolar disorder. The haplotype comprising g. −15503C/T and g. 16226G/A was most associated with bipolar disease ($p = 0.006$), but does not reach significant difference after multiple adjustments. One possible reason for not finding a significant association with bipolar disorder is that bipolar sample in the present study consists mostly of bipolar II patients ($n = 29$) rather than bipolar I patients ($n = 18$). Most studies of genetic linkage in bipolar disorder have samples that are predominantly bipolar I as this syndrome is more well defined. Further study with an increased number of samples is required to determine the contribution of this haplotype to the disease.

In the present study, we have identified a total of 42 polymorphisms as well as the precise LD pattern in *WFS1*. While some of the haplotypes of *WFS1* may be associated with type 2 diabetes or bipolar disorder, the data are inconclusive because of the small number in the study sample. Although the functional properties of the genetic variations in *WFS1* that might affect susceptibility to type 2 diabetes or bipolar disorder are not

known, the genetic variations and linkage disequilibrium patterns reported in this study should be useful in the investigation of the genetic associations between *WFS1* and various diseases, especially in Japanese.

Acknowledgments

This study was supported by Grants-in-Aid for Scientific Research A–C, and for Scientific Research on Priority Areas (C) "Medical Genome Science" from the Japanese Ministry of Science, Education, Sports, Culture and Technology; for a Health and Labor Science Research Grant for Special Research from the Japanese Ministry of Health, Labor and Welfare; and for the Yamanouchi Foundation for Research on Metabolic Disorders, and Takeda Science Foundation.

References

[1] D.J. Wolfram, H.P. Wagener, Diabetes mellitus and simple optic atrophy among siblings: report of four cases, Mayo Clin. Proc. 13 (1938) 715–718.
[2] R.G. Swift, D.B. Sadler, M. Swift, Psychiatric findings in Wolfram syndrome homozygotes, Lancet 336 (1990) 667–669.
[3] M.H. Polymeropoulos, R.G. Swift, M. Swift, Linkage of the gene for Wolfram syndrome to markers on the short arm of chromosome 4, Nat. Genet. 8 (1994) 95–97.
[4] D.A. Collier, T.G. Barrett, D. Curtis, A. Macleod, M.J. Arranz, J.A. Maassen, S. Bundey, Linkage of Wolfram syndrome to chromosome 4p16.1 and evidence for heterogeneity, Am. J. Hum. Genet. 59 (1996) 855–863.
[5] S. Nanko, H. Yokoyama, Y. Hoshino, H. Kumashiro, M. Mikuni, Organic mood syndrome in two siblings with Wolfram syndrome, Br. J. Psychiatry 16 (1992) 282.
[6] H. Inoue, Y. Tanizawa, J. Wasson, P. Behn, K. Kalidas, E. Bernal-Mizrachi, M. Mueckler, H. Marshall, H. Donis-Keller, P. Crock, D. Rogers, M. Mikuni, H. Kumashiro, K. Higashi, G. Sobue, Y. Oka, M.A. Permutt, A gene encoding a transmembrane protein is mutated in patients with diabetes mellitus and optic atrophy (Wolfram syndrome), Nat. Genet. 20 (1998) 143–148.
[7] T.M. Strom, K. Hortnagel, S. Hofmann, F. Gekeler, C. Scharfe, W. Rabl, K.D. Gerbitz, T. Meitinger, Diabetes insipidus, diabetes mellitus, optic atrophy and deafness (DIDMOAD) caused by mutations in a novel gene (wolframin) coding for a predicted transmembrane protein, Hum. Mol. Genet. 7 (1998) 2021–2028.
[8] K. Takeda, H. Inoue, Y. Tanizawa, Y. Matsuzaki, J. Oba, Y. Watanabe, K. Shinoda, Y. Oka, WFS1 (Wolfram syndrome 1) gene product: predominant subcellular localization to endoplasmic reticulum in cultured cells and neuronal expression in rat brain, Hum. Mol. Genet. 10 (2001) 477–484.
[9] T.G. Barrett, S.E. Bundey, A.F. Macleod, Neurodegeneration and diabetes: UK nationwide study of Wolfram (DIDMOAD) syndrome, Lancet 346 (1995) 1458–1463.
[10] A. Karasik, C. O'Hara, S. Srikanta, M. Swift, J.S. Soeldner, C.R. Kahn, R.D. Herskowitz, Genetically programmed selective islet beta-cell loss in diabetic subjects with Wolfram's syndrome, Diabetes Care 12 (1989) 135–138.
[11] R.G. Swift, M.H. Polymeropoulos, R. Torres, M. Swift, Predisposition of Wolfram syndrome heterozygotes to psychiatric illness, Mol. Psychiatry 3 (1998) 86–91.
[12] D.H. Blackwood, L. He, S.W. Morris, A. McLean, C. Whitton, M. Thomson, M.T. Walker, K. Woodburn, C.M. Sharp, A.F. Wright, Y. Shibasaki, D.M. St Clair, D.J. Porteous, W.J. Muir, A locus for bipolar affective disorder on chromosome 4p, Nat. Genet. 12 (1996) 427–430.
[13] P. Asherson, R. Mant, N. Williams, A. Cardno, L. Jones, K. Murphy, D.A. Collier, S. Nanko, N. Craddock, S. Morris, W. Muir, B. Blackwood, P. McGuffin, M.J. Owen, A study of chromosome 4p markers and dopamine D5 receptor gene in schizophrenia and bipolar disorder, Mol. Psychiatry 3 (1998) 310–320.
[14] J.L. Kennedy, F.M. Macciardi, Chromosome 4 workshop, Psychiatric Genet. 8 (1998) 67–71.
[15] F.H. Kooy, Hyperglycemia in mental disorders, Brain 42 (1919) 214–289.
[16] S.L. Lilliker, Prevalence of diabetes in a manic-depressive population, Compr. Psychiatry 21 (1980) 270–275.
[17] J.A. Gavard, P.J. Lustman, R.E. Clouse, Prevalence of depression in adults with diabetes. An epidemiological evaluation, Diabetes Care 16 (1993) 1167–1178.
[18] F. Cassidy, E. Ahearn, B.J. Carroll, Elevated frequency of diabetes mellitus in hospitalized manic-depressive patients, Am. J. Psychiatry 156 (1999) 1417–1420.
[19] W.T. Regenold, R.K. Thapar, C. Marano, S. Gavirneni, P.V. Kondapavuluru, Prevalence of type 2 diabetes mellitus among psychiatric inpatients with bipolar I affective and schizoaffective disorders independent of psychotropic drug use, J. Affect. Disord. 70 (2002) 19–26.
[20] APA, Diagnostic and Statistical Manual of Mental Disorders, 4th DSM-IV ed. Washington, DC: American Psychiatric Press, 1994.
[21] K. Cryns, T.A. Sivakumaran, J.M.W. Van den Ouweland, R.J.E. Pennings, C.W.R.J. Cremers, K. Flothmann, T.L. Young, R.J.H. Smith, M.M. Lesperance, G. Van Camp, Mutational spectrum of the WFS1 gene in Wolfram syndrome, nonsyndromic hearing impairment, diabetes mellitus, and psychiatric disease, Hum. Mutat. 22 (2003) 275–287.
[22] T. Awata, K. Inoue, S. Kurihara, T. Ohkubo, I. Inoue, T. Abe, H. Takino, Y. Kanazawa, S. Katayama, Missense variations of the gene responsible for Wolfram syndrome (WFS1/wolframin) in Japanese: possible contribution of the Arg456His mutation to type 1 diabetes as a nonautoimmune genetic basis, Biochem. Biophys. Res. Commun. 268 (2000) 612–616.
[23] J.A. Minton, A.T. Hattersley, K. Owen, M.I. McCarthy, M. Walker, F. Latif, T. Barrett, T.M. Frayling, Association studies of genetic variation in the WFS1 gene and type 2 diabetes in U.K. populations, Diabetes 51 (2002) 1287–1290.
[24] T. Ohtsuki, H. Ishiguro, T. Yoshikawa, T. Arinami, WFS1 gene mutation search in depressive patients: detection of five missense polymorphisms but no association with depression or bipolar affective disorder, J. Affect. Disord. 58 (2000) 11–17.
[25] T. Kato, K. Iwamoto, S. Washizuka, K. Mori, O. Tajima, T. Akiyama, S. Nanko, H. Kunugi, N. Kato, No association of mutations and mRNA expression of WFS1/wolframin with bipolar disorder in humans, Neurosci. Lett. 338 (2003) 21–24.

THE JOURNAL OF BIOLOGICAL CHEMISTRY
Vol. 279, No. 20, Issue of May 14, pp. 20915–20920, 2004
Printed in U.S.A.

Calpain System Regulates Muscle Mass and Glucose Transporter GLUT4 Turnover*

Received for publication, January 9, 2004, and in revised form, March 8, 2004
Published, JBC Papers in Press, March 9, 2004, DOI 10.1074/jbc.M400213200

Kenichi Otani‡, Dong-Ho Han‡, Eric L. Ford‡, Pablo M. Garcia-Roves‡, Honggang Ye§, Yukio Horikawa¶, Graeme I. Bell§‖, John O. Holloszy‡, and Kenneth S. Polonsky‡**

From the ‡Department of Medicine, Washington University School of Medicine, St. Louis, Missouri, 63110, the §Departments of Biochemistry and Molecular Biology and Medicine and the Howard Hughes Medical Institute, University of Chicago, Chicago, Illinois 60637, and the ¶Department of Cell Biology, Institute for Molecular and Cellular Regulation, Gunma University, Gunma 371–8512, Japan

The experiments in this study were undertaken to determine whether inhibition of calpain activity in skeletal muscle is associated with alterations in muscle metabolism. Transgenic mice that overexpress human calpastatin, an endogenous calpain inhibitor, in skeletal muscle were produced. Compared with wild type controls, muscle calpastatin mice demonstrated normal glucose tolerance. Levels of the glucose transporter GLUT4 were increased more than 3-fold in the transgenic mice by Western blotting while mRNA levels for GLUT4 and myocyte enhancer factors, MEF 2A and MEF 2D, protein levels were decreased. We found that GLUT4 can be degraded by calpain-2, suggesting that diminished degradation is responsible for the increase in muscle GLUT4 in the calpastatin transgenic mice. Despite the increase in GLUT4, glucose transport into isolated muscles from transgenic mice was not increased in response to insulin. The expression of protein kinase B was decreased by ~60% in calpastatin transgenic muscle. This decrease could play a role in accounting for the insulin resistance relative to GLUT4 content of calpastatin transgenic muscle. The muscle weights of transgenic animals were substantially increased compared with controls. These results are consistent with the conclusion that calpain-mediated pathways play an important role in the regulation of GLUT4 degradation in muscle and in the regulation of muscle mass. Inhibition of calpain activity in muscle by overexpression of calpastatin is associated with an increase in GLUT4 protein without a proportional increase in insulin-stimulated glucose transport. These findings provide evidence for a physiological role for calpains in the regulation of muscle glucose metabolism and muscle mass.

The presence of calpains, calcium-activated proteases, in mammalian cells was first reported over 30 years ago (1). Since that time at least 14 members of the calpain family have been identified and their chemistry and biology have been extensively studied (2). It has been proposed that alterations in calpain activity result in a number of disease states, including stroke (2, 3), traumatic brain injury (2, 3), Alzheimer's disease (2, 3), cataracts (3), limb-girdle muscular dystrophy (2, 3) and gastric cancer (2). Recent studies of the genetic basis of type 2 diabetes revealed that genetic variation in calpain 10 accounted for a significant component of the genetic risk for diabetes in a Mexican-American population (4). Subsequent studies have confirmed the role of calpain 10 as a diabetes susceptibility gene in some (5) but not all (6–13) populations studied.

The pathophysiological mechanism(s) whereby genetic variation in a calpain gene could lead to alterations in glucose tolerance are not known, and only a limited number of studies have examined the potential effects of alterations in calpain activity on insulin secretion or insulin action. These studies indicate that a reduction in calpain activity caused by calpain inhibitors induces a state of insulin resistance in isolated muscle strips (14). Pancreatic islets exposed to calpain inhibitors for 4–6 h demonstrated increased glucose-induced insulin secretion, whereas longer periods of exposure induced significant defects in insulin secretory responses to glucose and other secretagogues (14). These studies are limited by the fact that all experiments were conducted *in vitro*, and nonspecific effects of the calpain inhibitors, although unlikely, cannot be completely excluded. To examine the effects of inhibiting calpain activity using another *in vivo* experimental system, we produced transgenic mice that overexpress the endogenous calpain inhibitor, calpastatin.

EXPERIMENTAL PROCEDURES

Generation of MCK-hCAST Transgenic Mice—Full-length human calpastatin (hCAST)[1] corresponding to the 673-amino acid isoform described in GenBank™ accession number 1611327A was obtained using human pancreatic islet cDNA as template and amplified with forward and reverse primers 5′-TGG TGC AAC CAG CAA GTC TTC-3′ and 5′-GGA TGT TCA GAG ACT CAA C-3′, respectively. The PCR product was subcloned into pCR2.1-TOPO (Invitrogen) and the sequence of the insert confirmed. The insert was excised by digestion with EcoRI and cloned into the EcoRI site of the mouse muscle-specific creatine kinase (mMCK) promoter-bovine growth hormone (bGH) polyadenylation signal vector (15). The 4.28-kb mMCK-hCAST-bGH was excised from the vector by digestion with HhaI and purified by sucrose gradient centrifugation (Fig. 1). Transgenic mice were generated by microinjection of transgene DNA into the pronucleus of fertilized single-cell C57BL6 embryos at DNX Transgenic Sciences (Princeton, NJ). Animals were housed in a room maintained at 23 °C with a fixed 12-h light-dark cycle

* This work was supported in part by National Institutes of Health Grants DK18966 (to J. O. H.), DK31842 (to K. S. P.), and DK47486 and 20595 (to G. I. B.) as well as by the Diabetes Research and Training Center at Washington University. The costs of publication of this article were defrayed in part by the payment of page charges. This article must therefore be hereby marked "*advertisement*" in accordance with 18 U.S.C. Section 1734 solely to indicate this fact.

‖ An investigator of the Howard Hughes Medical Institute.
** To whom correspondence should be addressed: Dept. of Medicine, Washington University School of Medicine, 660 S. Euclid Ave., Campus Box 8066, St. Louis, MO 63110. Tel.: 314-362-8061; Fax: 314-362-8015; E-mail: polonsky@im.wustl.edu.

[1] The abbreviations used are: hCAST, human calpastatin; GLUT4, glucose transporter 4; MEF, myocyte enhancer factor; mMCK, mouse muscle-specific creatine kinase; EDL, extensor digitorum longus; WT, wild type; CsTg, calpastatin overexpression transgenic.

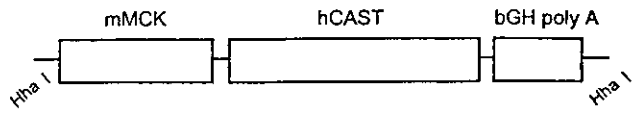

FIG. 1. **Transgene construct used in the production of the MCK-hCAST transgenic (CsTg) mice.**

and given free access to Purina chow and water. After an overnight fast, mice were anesthetized by an intraperitoneal injection of pentobarbital sodium (5 mg/100 g body weight), and the soleus, epitrochlearis, extensor digitorum longus (EDL), and other muscles were excised. All experimental procedures were approved by the Washington University Animal Study Committee.

DNA, RNA, and Protein Analysis—The mMCK-hCAST transgene was detected in transgenic mice by PCR analysis of tail DNA using forward and reverse primers 5′-GGC AAC GAG CTG AAA GCT CAT C-3′ and 5′-CAG TGA TAC CAG CAA CAC TCT CTC CAC C-3′. Total RNA was isolated from skeletal muscle using TRIzol reagent (Invitrogen) and suspended in Dnase- Rnase-free distilled water (Invitrogen). Mouse GLUT4 mRNA levels were determined by competitive RT-PCR using GLUT4 forward primer plus nested forward primer 5′-TCA ATG CCC CAC AGA AGG TGT CAA TGG TTG GGA AGG AAA AGG-3′ and reverse primer 5′-AAC CAG AAT GCC AAT GAC GAT G-3′ as described previously (34).

Total protein extracts were prepared by homogenizing muscle in 250 mM sucrose containing 20 mM HEPES and 1 mM EDTA, pH 7.4. Protein was resolved by SDS-PAGE and transferred to nitrocellulose membranes (Amersham Biosciences). The membranes were blocked overnight at 4 °C with 5% nonfat milk in phosphate-buffered saline containing 0.1% Tween 20. The membranes were probed with the following primary antibodies: polyclonal anti-CAST (Calbiochem, La Jolla, CA), anti-GLUT1 and -GLUT4 (a generous gift from Dr. Mike Mueckler, Washington University), anti-MEF 2A (Santa Cruz Biotechnology, Santa Cruz, CA), and anti-MEF 2D (Transduction Laboratories, Lexington, KY) as well as anti-insulin receptor β subunit, anti-insulin receptor substrate-1, anti-insulin receptor substrate-2, monoclonal anti-Akt/PKB, and anti-phosphatidylinositol 3-kinase, all from Upstate Cell Signaling Solution, Lake Placid, NY. Horseradish peroxidase-conjugated secondary antibodies were obtained from Jackson ImmunoResearch Laboratories (West Grove, PA), and reagents for enhanced chemiluminescence were obtained from Amersham Biosciences.

Physiological Studies—Intraperitoneal glucose tolerance tests were performed following a 4-h fast. Blood was sampled from the tail vein prior to and 30, 60, and 120 min after injection of dextrose intraperitoneally (2 g/kg body weight). For glucose transport studies, epitrochlearis, soleus, and EDL muscles were removed and allowed to recover from dissection by incubation in 2 ml of Krebs-Henseleit buffer (KHB) containing 8 mM glucose, 32 mM mannitol, and 0.1% bovine serum albumin for 1 h at 35 °C in a shaking incubator. This was followed by 30 min of incubation in the same medium with or without a maximally effective insulin concentration (2 microunits/ml). The gas phase during the incubation was 95% O_2, 5% CO_2. The muscles were then washed for 10 min in KHB containing 40 mM mannitol, 0.1% bovine serum albumin, and insulin (if it was present in the previous incubation) to remove glucose from the extracellular space. Muscles were then transferred to 1.5 ml of KHB containing 3 mM 2-deoxy-D-[1,2-^{3}H]glucose (2DG) (1.5 μCi/ml), 36 mM [^{14}C]mannitol (0.2 μCi/ml), 0.1% bovine serum albumin, and insulin (if it was present in the previous incubation). Extracellular space and intracellular 2DG concentration were then determined as described previously (16).

Measurement of Muscle Weight—The soleus, EDL, tibialis anterior, gastrocnemius, and quadriceps muscles were dissected out using a consistent surgical approach. The muscles were weighed immediately following dissection after blood had been removed from the muscle surface.

Measurement of Muscle Glycogen Content—Glycogen content was measured in perchloric acid extracts of muscle by the amyloglucosidase method (17).

In Vitro Cleavage of Human GLUT4 by Calpain-2—Human GLUT4 (hGLUT4) protein was prepared using a coupled *in vitro* transcription and translation system (Promega, Madison, WI). One microgram of the hGLUT4-plasmid construct pGEM4Z-AMT7 (18) was incubated in the coupled transcription and translation reaction with 20 μCi of [^{35}S]Met in a volume of 50 μl to generate [^{35}S]-labeled hGLUT4. Unlabeled hGLUT4 was prepared by using 20 μM Met in the coupled transcription and translation reaction. Four microliters of the coupled transcription and translation reaction was incubated with 1.7 units of recombinant rat calpain-2 (Calbiochem) in 20 μl of calpain cleavage buffer (150 mM NaCl, 20 mM Tris-HCl (pH 7.4), 1 mM dithiothreitol, and 0.1% bovine serum albumin). Calpain was activated by addition of $CaCl_2$ to 5 mM. Cleavage was terminated after 5 and 30 min by addition of 20 μl of SDS-sample buffer (0.125 M Tris-HCl (pH 6.8), 4% SDS, 20% glycerol, 0.2 M dithiothreitol, and 0.02% bromphenol blue). Samples were heated at 55 °C for 15 min and analyzed on a 4–20% SDS-PAGE followed by autoradiography or Western blotting. The Western blot was developed using a polyclonal anti-GLUT4 antibody generated using a cytoplasmic 12-amino acid C-terminal peptide from mouse GLUT4 (Alpha Diagnostic, San Antonio, TX).

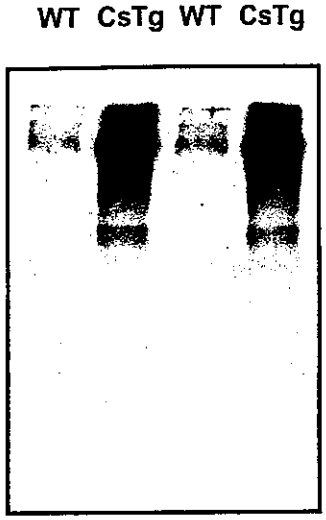

FIG. 2. **Muscle calpastatin expression.** Overexpression of human calpastatin in muscles of CsTg but not WT mice was confirmed by Western blot.

RESULTS

Generation of Transgenic Mice Overexpressing Calpastatin in Muscle—We obtained five founders (two females and three males). Human calpastatin was expressed in muscle (soleus and EDL) from all five founders. The founder used to generate the mice used in the present experiments showed a substantially greater level of calpastatin expression (~20-fold) than the other founders, which all showed a similar level of overexpression. All transgenic mice were heterozygous. All were used around 4 months of age.

Calpastatin Expression by Western Blot—Overexpression of human calpastatin in muscles was confirmed by Western blot (Fig. 2). Although human calpastatin was not expressed in muscle from WT mice, substantial expression was detected in transgenic (CsTg) mice.

Mouse Body Weight and Glucose Tolerance—The body weights of male WT mice averaged 28.1 ± 0.6 g compared with 31.2 ± 0.5 g for the CsTg group ($p < 0.01$, 8 mice per group, 23–25 weeks old). For the female mice, body weight averaged 21.8 ± 0.3 g for the WT group and 23.2 ± 0.4 g for the CsTg group ($p < 0.01$, n = 16 per group, 23–25 weeks old). Differences in the intraperitoneal glucose tolerance test between the WT and the CsTg mice (WT *versus* CsTg: 182.3 ± 6.9 mg/dl *versus* 197.9 ± 9.3 mg/ dl at fasting, 189.3 ± 7.0 mg/ dl *versus* 198.3 ± 10.0 mg/ dl at 2 h after injection) were not statistically significant.

Insulin Action in Muscle from CsTg Mice—The increase in 2-deoxy-D-[1,2-^{3}H] glucose transport in response to a maximally effective insulin concentration (2 microunits/ml) was not significantly different in muscles from CsTg mice as compared with the WT controls in either EDL (Fig. 3), soleus (data not shown), or epitrochlearis (data not shown). Basal rates of glucose transport were also not different.

GLUT4 Glucose Transporter Expression—As shown in Fig. 4, GLUT4 protein content of EDL, soleus, triceps, and tibialis

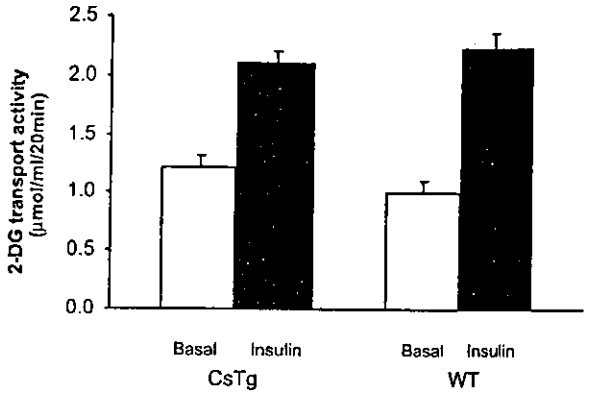

FIG. 3. **Insulin-stimulated 2-deoxyglucose transport.** EDL muscles were incubated in the absence or presence of insulin (2 microunits/ml). Values shown are means ± S.E. for seven muscles per group. There were no significant differences between the WT and the CsTg mice.

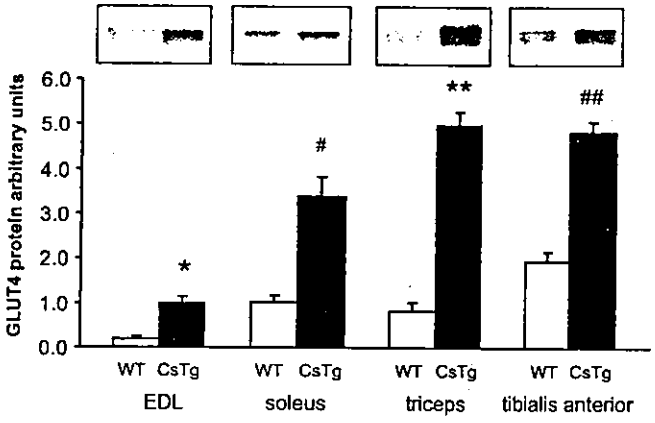

FIG. 4. **Measurement of immunoreactive GLUT4.** GLUT4 protein was determined by Western blotting in EDL, soleus, triceps, and tibialis anterior using a rabbit polyclonal antibody directed against the C terminus of GLUT4. Values are means ± S.E. for eight muscles per group. *, $p < 0.001$; **, $p < 0.0001$; #, $p < 0.00001$; ##, $p < 0.000002$ *versus* WT mice.

anterior muscles was increased more than 3-fold in CsTg mice. The magnitude of insulin-stimulated muscle glucose transport is normally directly proportional to muscle GLUT4 content. This relationship is evident when muscle fiber types with different GLUT4 contents are compared (19), and in muscles that have undergone an adaptive increase in GLUT4 protein (20–22). Thus, the finding that stimulated glucose transport was the same in the CsTg as in the WT muscles despite 3-fold increases in the GLUT4 protein indicates that the increase in GLUT4 protein associated with calpastatin overexpression did not cause the expected increase in glucose transport in response to stimulation by insulin.

GLUT4 mRNA Levels—Increases in GLUT4 expression induced by various adaptive stimuli may be mediated at the transcriptional level, as evidenced by an increased GLUT4 mRNA (23). However, GLUT4 mRNA was significantly decreased in muscles from CsTg mice (Fig. 5), suggesting that the increase in GLUT4 protein was mediated by a post-transcriptional mechanism. Further support for this hypothesis is provided by the finding that MEF 2A and MEF 2D protein levels were decreased ~50% in the CsTg muscles. Expression of GLUT4 in striated muscle is dependent on binding of a MEF 2A-MEF 2D heterodimer to the GLUT4 promoter (24). We have found that stimuli that induce increased GLUT4 expression also result in increases in MEF 2A and MEF 2D (25). As shown in Fig. 6, *A* and *B*, both MEF 2A and MEF 2D were significantly

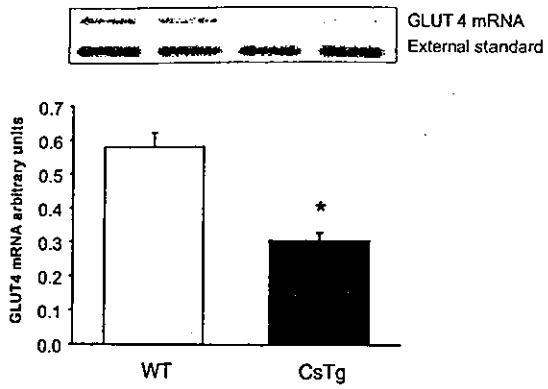

FIG. 5. **Measurement of GLUT4 mRNA.** The sequence of competitor RNA was identical to cDNA amplified by RT-PCR except for a 155-bp internal deletion (161–315). Mouse skeletal muscle total RNA was reverse-transcribed into cDNA and amplified using hybrid forward primer and reverse primer. Values are means ± S.E. for eight muscles per group. *, $p < 0.003$.

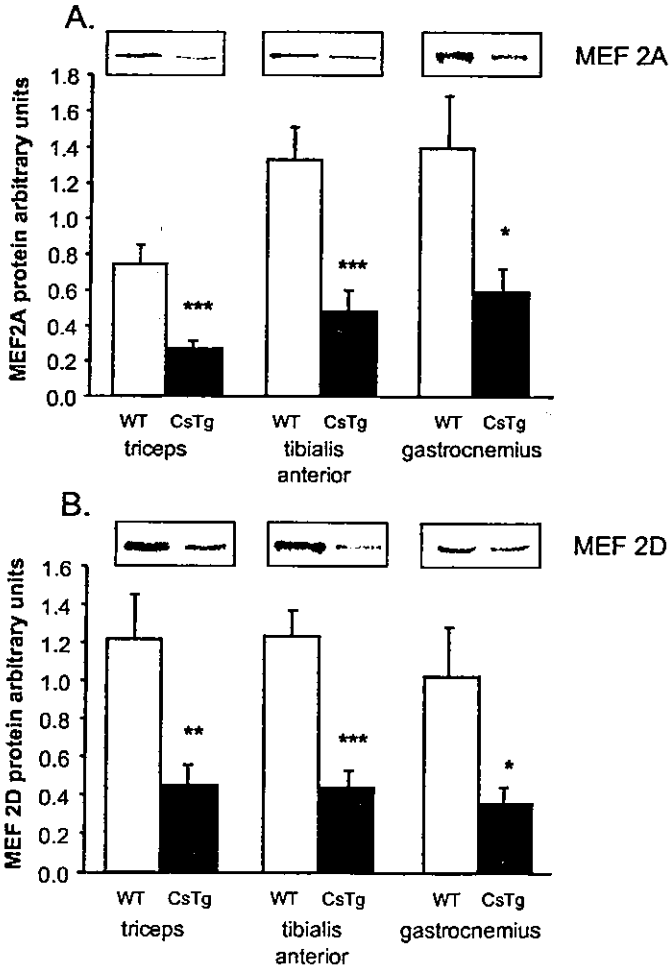

FIG. 6. **Measurement of immunoreactive MEF 2A and 2D.** *A*, MEF 2A. *B*, MEF 2D. Myocyte enhancer factors MEF 2A and 2D were measured by Western blot. Expression of GLUT4 in striated muscle is dependent on binding of MEF 2A-2D heterodimer to the GLUT4 promoter. Values are means ± S.E. Triceps ($n = 8$), tibialis anterior ($n = 8$), and gastrocnemius ($n = 6$). *, $p < 0.05$; **, $p < 0.01$; ***, $p < 0.001$.

decreased in muscles from CsTg mice compared with WT controls.

GLUT1 Glucose Transporter Expression—The finding that GLUT4 protein is increased in muscles of the CsTg mice, despite a decrease in GLUT4 mRNA, led us to hypothesize that GLUT4 is a calpain substrate and that inhibition of calpain by

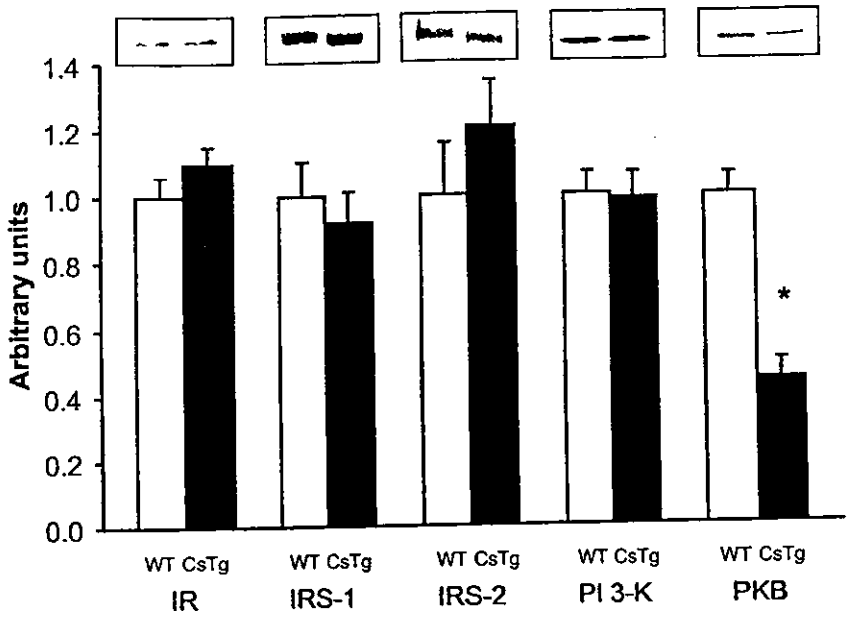

FIG. 7. **Measurement of immunoreactive insulin receptor (*IR*), insulin receptor substrates (*IRS*) -1 and -2, protein kinase B (*PKB*), and phosphatidylinositol 3-kinase (*PI 3-K*).** Values are means ± S.E. (n = 6, gastrocnemius muscle); *, p <0.0006.

calpastatin is responsible for the increase in GLUT4. If this hypothesis is correct, one might also expect to see an increase in GLUT1 protein because its amino acid sequence is similar to that of GLUT4 (26). We, therefore, measured the GLUT1 protein level and found that it was also increased in skeletal muscle of the CsTg mice. Although highly significant (controls, 1.04 ± 0.14 *versus* CsTg, 1.66 ± 0.14 arbitrary units, mean ± S.E. for 16 muscles per group, p <0.004), the magnitude of the increase was smaller than that of GLUT4.

Muscle Glycogen—Glucose transport is the primary rate-limiting step that determines the rate and extent of muscle glycogen accumulation (27). Increases in muscle GLUT4 are, therefore, generally associated with an increase in muscle glycogen content (20–22, 28, 29). Muscle glycogen concentrations were significantly increased in muscles of the CsTg mice, 20.4 ± 0.9 μmol/g EDL WT muscle compared with 46.0 ± 2.7 μmol/g EDL CsTg muscle.

Effect of Muscle Glycogen Depletion on Glucose Transport—Accumulation of glycogen in muscle may induce insulin resistance. To determine whether the increase in glycogen in muscles from CsTg mice was masking an increase in muscle glucose transport in CsTg muscles, we exposed muscles to hypoxia for 80 min, a maneuver that reduces glycogen. The glucose concentration in the incubation medium for the CsTg muscles was also reduced compared with the incubations for the WT muscles (2 and 8 mM glucose, respectively). This approach markedly reduced glycogen concentrations to ~7 μmol/g muscle wet weight. However, even after a reduction in muscle glycogen there were no significant differences in glucose transport induced by 2 microunits/ml insulin and hypoxia in the EDL and the soleus muscles of the CsTg compared with the WT mice (data not shown). Thus, the increase in GLUT4 resulting from calpain inhibition was not associated with a parallel increase in muscle glucose transport.

Proteins of the Insulin Signaling Pathway—As a next step in our investigation of the mechanism responsible for the relative insulin resistance of the CsTg muscles, we measured the levels of some of the proteins of the insulin signaling pathway. Expression of the insulin receptor, insulin receptor substrates 1 and 2, and phosphatidylinositol 3-kinase proteins was similar in skeletal muscle of the transgenic and wild type mice (Fig. 7). However, there was a remarkable (~60%) decrease in protein kinase B in skeletal muscle of the CsTg mice (Fig. 7). This finding could explain why insulin-stimulated glucose transport is not increased in CsTg muscle despite a ~3-fold increase in GLUT4.

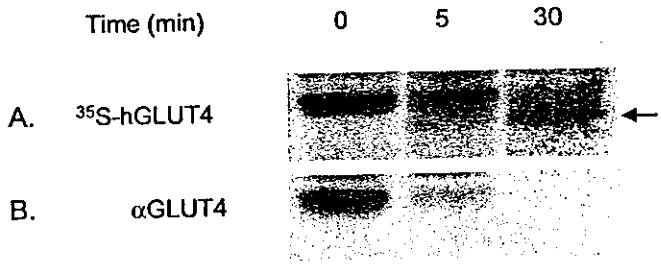

FIG. 8. **Human GLUT4 is cleaved by calpain-2 *in vitro*.** *A*, ^{35}S-labeled recombinant hGLUT4 was incubated with calpain-2 for 5 and 30 min. The samples were subjected to SDS-PAGE and autoradiography. *B*, unlabeled recombinant GLUT4 was incubated with calpain-2. The GLUT4 protein was identified by Western blot using an anti-C-terminal GLUT4 antibody (*αGLUT4*). The *arrowhead* indicates the GLUT4 fragment generated on incubation with calpain-2.

Cleavage of Human GLUT4 in Vitro by Calpain-2—To determine whether human GLUT4 is a calpain cleavage substrate, we incubated ^{35}S-labeled recombinant hGLUT4 with purified calpain-2. The recombinant hGLUT4 has a mass of 43.7 kDa, and incubation with activated calpain-2 generated a protein with an estimated mass of 37.2 kDa (Fig. 8*A*). This fragment was not identified by an antibody that binds to an epitope at the C terminus of GLUT4 (Fig. 8*B*), suggesting the calpain-2 cleavage site is located in the C-terminal portion of GLUT4. The mass of the cleavage product suggests that the calpain-sensitive site is about 60–70 residues from the C terminus.

Effects on Muscle Mass—To determine whether overexpression of calpastatin affected muscle mass, muscles were systematically weighed in 23–25-week-old mice. Weight of EDL and soleus muscles was increased 12% (EDL, males), 33% (EDL, females), 17% (soleus, males), and 19% (soleus, females), respectively (Fig. 9*A*). Similar increases in mass were present in the other muscles, including the tibialis anterior (42% in males, 47% in females), gastrocnemius (13% in males, 14% in females), and quadriceps (21% in males, 14% in females) (Fig. 9*B*). Total muscle protein was increased in proportion to muscle weight in EDL (WT *versus* CsTg: 1.96 ± 0.10 mg *versus* 2.40 ± 0.10 mg, p <0.01) and soleus (WT *versus* CsTg: 1.58 ± 0.08 mg *versus* 1.85 ± 0.10 mg, p <0.05).

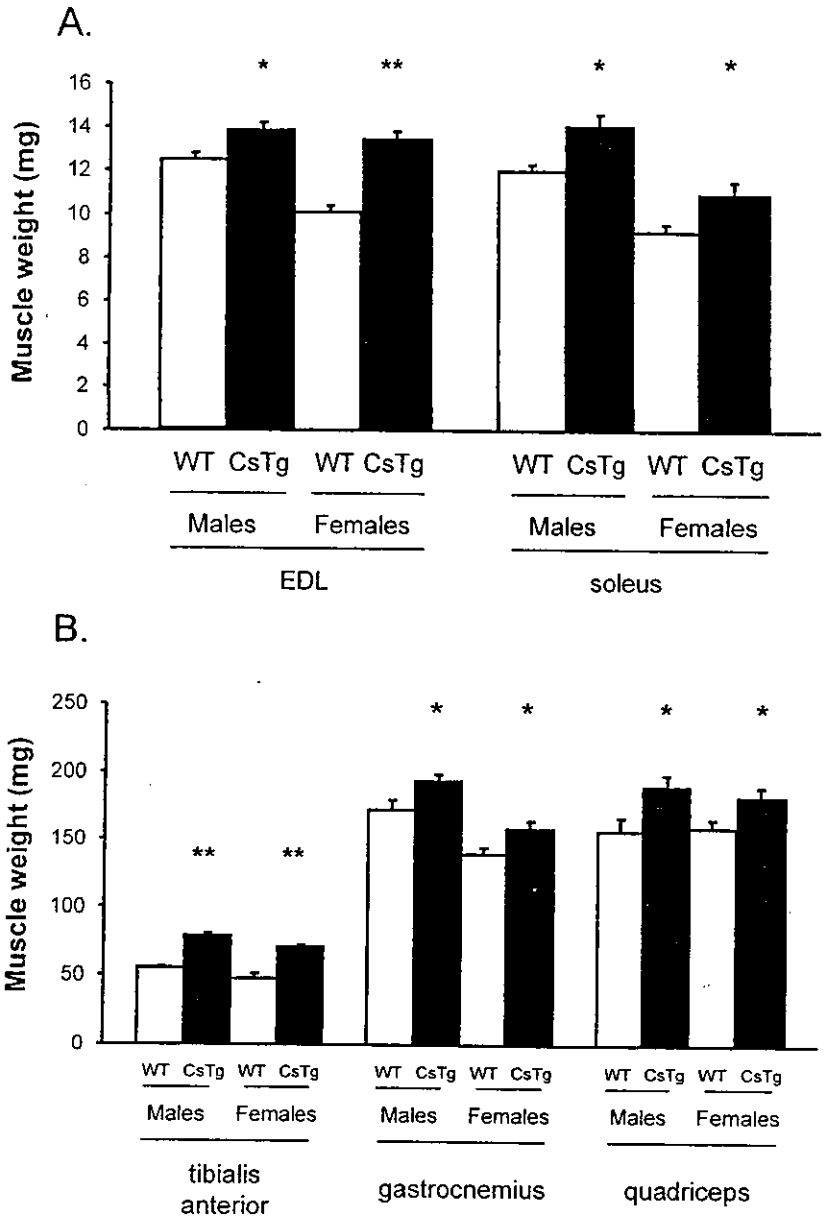

FIG. 9. **Muscle weight.** Muscles of 23–25-week-old mice were carefully dissected and weighed. Values are means ± S.E. for six to eight muscles per group. *, $p < 0.05$; **, $p < 0.0001$.

DISCUSSION

The present study was designed to determine whether reducing calpain expression in muscle is associated with alterations in muscle glucose metabolism. A transgenic mouse with muscle-specific overexpression of calpastatin was used as the experimental model. The transgenic mice did not have overt changes in glucose tolerance and did not appear to be insulin-resistant *in vivo*. However, *in vitro* studies of muscle revealed a number of interesting effects of calpastatin overexpression.

One important change observed was a greater than 3-fold increase in GLUT4 protein detected by Western blotting. The increase was found consistently in a number of different muscles, including EDL, soleus, triceps, and tibialis anterior. It is most likely that the increase in GLUT4 is due to a reduction in the rate of GLUT4 breakdown for the following reasons. GLUT4 mRNA was not increased and was actually decreased, as were protein levels for MEF 2A and 2D, two transcription factors that mediate induction of GLUT4 expression (24). Our hypothesis is that GLUT4 serves as a calpain substrate and that the reduction in calpain activity resulting from increased expression of calpastatin leads to the increase in GLUT4 levels observed. The results of additional experiments that demonstrated that GLUT4 is a substrate for calpain-2 *in vitro* are consistent with this idea, as is the finding that GLUT1, which has an amino acid sequence similar to that of GLUT4 (26), was also increased.

Previous experiments have shown that pharmacological inhibition of calpain causes insulin resistance of glucose transport in skeletal muscle (14). In view of this observation, we expected that overexpression of calpastatin, an endogenous calpain inhibitor, would result in severe skeletal muscle insulin resistance. Our finding that insulin-stimulated glucose transport was normal in CsTg muscles provides evidence suggesting that the greater than 3-fold increase in GLUT4 protein induced by calpastatin overexpression compensated for insulin resistance caused by inhibition of calpain activity. Maximally insulin-stimulated glucose transport is normally directly proportional to the GLUT4 protein content of a muscle (19, 21, 22). Therefore, the finding that glucose transport rates were the same in muscles of the WT and CsTg mice, despite the higher GLUT4 content of the CsTg muscles, provides evidence for a severe resistance to stimulation of glucose transport of the CsTg muscles relative to their GLUT4 content. Our finding of an ~60% reduction in protein kinase B expression in CsTg

skeletal muscle raises the possibility that an attenuation of insulin signaling via this step may play a role in mediating the relative insulin resistance. The marked decrease in expression of MEF 2A, MEF 2D, and protein kinase B provides evidence suggesting that the large increase in GLUT4 directly or by means of a secondary effect, such as the increase in glycogen, results in suppression of the expression of these proteins.

It used to be thought that calpains play a major role in muscle protein degradation only when cytosolic Ca^{2+} homeostasis is disturbed by trauma or ischemia and in muscular dystrophies (30, 31). The role of calpains in protein turnover in normal skeletal muscle is still unclear. However, evidence is accumulating that calpains mediate the initiating steps in the turnover of myofibrillar proteins. It appears that calpains are responsible for release of filaments from the myofibrils, making them available for degradation by the proteasome (32). It was recently reported that overexpression of calpastatin in skeletal muscle protects mice against the muscle atrophy associated with hindlimb unloading (33). The present finding that calpastatin overexpression results in skeletal muscle hypertrophy provides evidence that calpains are also involved in normal skeletal muscle protein turnover.

The implications of the results of this study for our understanding of the pathophysiology of type 2 diabetes are unclear. Genetic variation in a specific calpain, calpain 10, has been associated with altered risk for type 2 diabetes (4, 5). Although calpastatin inhibits the activity of calpains I and II, it has not been determined whether it has similar effects on calpain 10. Nevertheless, our results provide further evidence that inhibition of calpain activity causes insulin resistance. This finding implies that calpain plays a role in the stimulation of glucose transport. Our results also provide additional new information indicating that inhibition of calpain activity in skeletal muscle results in an increase in GLUT4 protein and causes muscle hypertrophy. These findings strongly suggest that calpains play important roles in GLUT4 and skeletal muscle proteolysis.

Acknowledgment—The support of the Kovler Foundation is gratefully acknowledged.

REFERENCES

1. Guroff, G. (1964) *J. Biol. Chem.* **239,** 149–155
2. Haung, Y., and Wang, K. K. W. (2001) *Trends Mol. Med.* **7,** 355–362
3. Wang, K. K. W., and Yuen, P.-W. (1997) *Trends Pharmacol. Sci.* **15,** 412–419
4. Horikawa, Y., Oda, N., Cox, N. J., Li, X., Melander, M. O., Hara, M., Hinokio, Y., Lindner, T. H., Mashima, H., Schwarz, P. E. H., Plata, L. B., Horikawa, Y., Oda, Y., Yoshiuchi, I., Colilla, S., Polonsky, K. S., Wei, H., Concannon, P., Iwasaki, N., Shulze, J., Baier, L. J., Bogardus, C., Groop, L., Boerwinkle, E., Hanis, C. L., and Bell, G. I. (2000) *Nat. Genet.* **26,** 163–175
5. Hanis, C. L., Boerwinkle, E., Chakraborty, R., Ellsworth, D. L., Concannon, P., Stirling, B., Morrison, V. A., Wapelhorst, B., Spielman, R. S., Gogolin-Ewens, K. J., Shepard, J. M., Williams, S. R., Risch, N., Hinds, D., Iwasaki, N., Ogata, M., Omori, Y., Petzold, C., Reitzch, H., Schroder, H. E., Schulze, J., Cox, N. J., Menzel, S., Boriraj, V. V., Chen, X., Lim, L. R., Linder, T., Mereu, L. E., Wang, Y. Q., Xiang, K., Yamagta, K., Yang, Y., and Bell, G. I. (1996) *Nat. Genet.* **13,** 161–166
6. Duggirala, R., Blangero, J., Aomasy, L., Dyer, T. D., Williams, K. L., Leach, R. J., O'Connell, P., and Stern, M. P. (1999) *Am. J. Hum. Genet.* **64,** 1127–1140
7. Mahtani, M. M., Widen, E., Lehto, M., Thomas, J., McCarthy, M., Brayer, J., Bryant, B., Gayun, C., Daly, M., Forsblom, C., Kanninen, T., Kirby, A., Kruglyak, L., Munnelly, K., Parkkonen, M., Reeve-Daly, M. P., Weaver, A., Brettin, T., Duyk, G., Lander, E. S., and Groop, L. C. (1996) *Nat. Genet.* **14,** 90–94
8. Harson, R. L., Ehm, M. G., Pettitt, D. J., Prochazka, M., Thompson, D. B., Timberlake, D., Foroud, T., Kobes, S., Baier, L., Burns, D. K., Almasy, L., Blangero, J., Garvey, W. T., Bennett, P. H., and Knowler, W. C. (1998) *Am. J. Hum. Genet.* **63,** 1130–1138
9. Elbein, S. C., Hoffman, M. D., Teng, K., Leppert, M. F., and Hasstedt, S. J. (1999) *Diabetes* **48,** 1175–1182
10. Hani, E. H., Hager, J., Philippi, A., Demenais, F., Froguel, P., and Vionnet, N. (1997) *Diabetes* **46,** 1225–1226
11. Thomas, A. W., Sherratt, E. J., Gagg, J. W., Davies, S. A., Majid, A., and Alcolado, J. C. (1997) *Hum. Genet.* **101,** 212–213
12. Ciccarese, M., Tonolo, G., Delin, I., Wong, F. K., Holm, P., Atzeni, M. M., Lichtenstein, P., Kockum, I., Maioli, M., and Luthman, H. (1997) *Diabetologia* **40,** 1366–1367
13. Ghosh, S., Hauser, E. R., Magnuson, V. L., Valle, T., Ally, D. S., Karanjawala, Z. E., Rayman, J. B., Knapp, J. I., Musick, A., Tannenbaum, J., Te, C., Eldridge, W., Shapiro, S., Musick, T., Martin, C., So, A., Witt, A., Harvan, J. B., Watanabe, R. M., Hagopian, W., Eriksson, J., Nylund, S. J., Kohtamaki, K., Tuomilehto-Wolf, E., Toivanen, L., Vidgren, G., Ehnholm, C., Bergman, R. N., Tuomilehto, J., Collins, F. S., and Boehnke, M. (1998) *J. Clin. Investig.* **102,** 704–709
14. Sreenan, S. K., Zhou, Y. P., Otani, K., Hansen, P. A., Currie, K. P. M., Pan, C. Y., Lee, J. P., Ostrega, D. M., Pugh, W., Horikawa, Y., Cox, N. J., Hanis, C. L., Burant, C. F., Fox, A. P., Bell, G. I., and Polonsky, K. S. (2001) *Diabetes* **50,** 2013–2020
15. Zhu, X., Hadhazy, M., Groh, M. E., Wheeler, M. T., Wollmann, R., and McNally, E. M. (2001) *J. Biol. Chem.* **276,** 21785–21790
16. Young, D. A., Uhl, J. J., Cartee, G. D., and Holloszy, J. O. (1986) *J. Biol. Chem.* **261,** 16049–16053
17. Passonneau, J. V., and Lauderdale, V. R. (1974) *Anal. Biochem.* **60,** 405–412
18. Fukumoto, H., Kayno, T., Buse, J. B., Edwards, Y., Pilch, P. F., Bell, G. I., and Seino, S. (1989) *J. Biol. Chem.* **264,** 7776–7779
19. Henriksen, E. J., Bourey, R. E., Rodnick, K. J., Koranyi, L., Permutt, M. A., and Holloszy, J. O. (1990) *Am. J. Physiol.* **259,** E593-E598
20. Weinstein, S. P., Watts, J., and Haber, R. S. (1991) *Endocrinology* **129,** 455–464
21. Ren, J. M., Semenkovich, C. F., and Holloszy, J. O. (1993) *Am. J. Physiol.* **264,** C146-C150
22. Ren, J.-M., Semenkovich, C. F., Gulve, E. A., Gao, J., and Holloszy, J. O. (1994) *J. Biol. Chem.* **269,** 14396–14401
23. MacLean, P. S., Zheng, D., Jones, J. P., Olson, A. L., and Dohm, G. L. (2002) *Biochem. Biophys. Res. Commun.* **292,** 409–414
24. Mora, S., and Pessin, J. E. (2000) *J. Biol. Chem.* **275,** 16323–16328
25. Ojuka, E. O., Jones, T. E., Nolte, L. A., Chen, M., Wamhoff, B. R., Sturek, M., and Holloszy, J. O. (2002) *Am. J. Physiol.* **282,** E1008-E1013
26. Mueckler, M. (1994) *Eur. J. Biochem.* **219,** 713–725
27. Ren, J. M., Marshall, B. A., Gulve, E. A., Gao, J., Johnson, D. W., Holloszy, J. O., and Mueckler, M. (1993) *J. Biol. Chem.* **268,** 16113–16115
28. Hansen, P. A., Gulve, E. A., Marshall, B. A., Gao, J., Pessin, J. E., Holloszy, J. O., and Mueckler, M. (1995) *J. Biol. Chem.* **270,** 1679–1684
29. Greiwe, J. S., Hickner, R. C., Hansen, P. A., Racette, S. B., Chen, M. M., and Holloszy, J. O. (1999) *J. Appl. Physiol.* **87,** 222–226
30. Lecker, S. H., Solomon, V., Mitch, W. E., and Goldberg, A. L. (1999) *J. Nutr.* **129,** 227S-237S
31. Tidball, J. G., and Spencer, J. M. (2000) *Int. J. Biochem. Cell Biol.* **32,** 1–5
32. Goll, D. E., Thompson, V. F., Li, H., Wei, W., and Cong, J. (2003) *Physiol. Rev.* **83,** 731–801
33. Tidball, J. G., and Spencer, M. J. (2002) *J. Physiol.* **545,** 819–828
34. Garcia-Roves, P. M., Han, D.-H., Song, Z., Jones, T. E., Hucker, K. A., and Holloszy, J. O. (2003) *Am. J. Physiol.* **285,** E729–E736

THE JOURNAL OF BIOLOGICAL CHEMISTRY
© 2004 by The American Society for Biochemistry and Molecular Biology, Inc.

Vol. 279, No. 23, Issue of June 4, pp. 24794–24802, 2004
Printed in U.S.A.

RyR2 and Calpain-10 Delineate a Novel Apoptosis Pathway in Pancreatic Islets*

Received for publication, February 4, 2004, and in revised form, March 8, 2004
Published, JBC Papers in Press, March 25, 2004, DOI 10.1074/jbc.M401216200

James D. Johnson‡§, Zhiqiang Han‡, Kenichi Otani‡, Honggang Ye¶, Yan Zhang‡, Hong Wu‖, Yukio Horikawa, Stanley Misler‡, Graeme I. Bell¶, and Kenneth S. Polonsky‡ ‡‡**

*From the ‡Department of Internal Medicine, Washington University, St. Louis, Missouri 63110, ¶Department of Biochemistry, University of Chicago, Chicago, Illinois 60637, ‖Department of Pharmacology, University of California, Los Angeles, California 90210, and **Department of Cell Biology, Gunma University, Gunma 371-8511, Japan*

Cells are programmed to die when critical signaling and metabolic pathways are disrupted. Inhibiting the type 2 ryanodine receptor (RyR2) in human and mouse pancreatic β-cells markedly increased apoptosis. This mode of programmed cell death was not associated with robust caspase-3 activation prompting a search for an alternative mechanism. Increased calpain activity and calpain gene expression suggested a role for a calpain-dependent death pathway. Using a combination of pharmacological and genetic approaches, we demonstrated that the calpain-10 isoform mediated ryanodine-induced apoptosis. Apoptosis induced by the fatty acid palmitate and by low glucose also required calpain-10. Ryanodine-induced calpain activation and apoptosis were reversed by glucagon-like peptide or short-term exposure to high glucose. Thus RyR2 activity seems to play an essential role in β-cell survival *in vitro* by suppressing a death pathway mediated by calpain-10, a type 2 diabetes susceptibility gene with previously unknown function.

The pancreatic β-cell plays a central role in the pathogenesis of diabetes mellitus. A reduction in β-cell mass mediated at least in part by an increase in apoptosis is characteristic of the diabetic state (1–3). It is becoming clear that several pathways can lead to β-cell apoptosis, including cytokine signaling, excessive Ca^{2+} influx during chronic hyperglycemia, high levels of free fatty acids, hypoxia or hypoglycemia, endoplasmic reticulum (ER)[1] stress, and loss of growth factor signaling (1, 3–12). Whether various inducers of apoptosis employ distinct molecular mechanisms has not been systematically studied.

Intracellular Ca^{2+} stores play an important role in the regulation of apoptosis in many cell types (13, 14). The present study was undertaken to test the hypothesis that alterations in specific intracellular Ca^{2+} stores may induce apoptosis in pancreatic β-cells. There are at least three classes of intracellular Ca^{2+} stores in β-cells, and these are sensitive, respectively, to inositol trisphosphate (IP_3)/thapsigargin, nicotinic acid adenine dinucleotide phosphate, and cyclic ADP ribose/ryanodine (15–18). In many cell types, ryanodine receptor Ca^{2+} channels (RyR) transmit Ca^{2+} signals directly to closely associated mitochondria (19). In the MIN6 β-cell line, RyR were shown to regulate ATP production (20). Because of their role in regulating intracellular Ca^{2+} and mitochondrial function, we focused specifically on RyR as likely mediators of β-cell apoptosis. Of the three RyR subtypes, two have been reported to be present in β-cells, RyR1 and RyR2. The latter is more abundant and can be distinguished from the former by its insensitivity to dantrolene (21, 22). Ryanodine, a plant alkaloid, is the most specific probe for all RyR subtypes, and its activity is lost in RyR-deficient cells (23, 24).

In the present study, we examined the role of RyR in the survival of human and mouse pancreatic islets. We uncovered a novel apoptosis pathway that is initiated when Ca^{2+} flux through RyR2 is blocked. The mechanism of ryanodine-induced programmed cell death shares important features with palmitate-induced apoptosis, and both require activation of calpain-10, a type 2 diabetes susceptibility gene.

MATERIALS AND METHODS

Reagents—High purity ryanodine, dantrolene, ALLM and DEVD-CHO were purchased from Calbiochem (La Jolla, CA) and kept as 1000× stocks in Me_2SO. Thapsigargin (Calbiochem) was dissolved in ethanol (ETOH). Palmitate was in dissolved ETOH/NaOH at 55 °C. Human glucagon-like-peptide 1 (GLP-1) was purchased from Peninsula Lab (San Carlos, CA).

Immunofluorescence Staining—Ryanodine receptors were detected using a monoclonal antibody that recognizes RyR1 and RyR2 (Affinity BioReagents, Golden, CO). For double-labeling experiments, insulin staining was performed using guinea pig anti-insulin antibody (Linco, St. Charles, MO). Secondary antibodies conjugated to either Alexa Fluor 488 or 596 were applied for 2 h. Controls using no primary antibody or no second antibody were negative for each experiment. A FluoView™ laser scanning confocal microscope (Olympus, Melville, NY) was used for studies of RyR localization.

Cell Culture and Ca^{2+} Imaging—Human islets were obtained from the Washington University Human Islet Isolation Core Lab. Standard culturing methods were employed as described for human islets (16), mouse islets (1), and MIN6 cells (9) using RPMI 1640 media (with 10% fetal calf serum, 100 units/ml penicillin, and 100 μg/ml streptomycin). RPMI 1640 medium contained 10 mM glucose unless otherwise indicated. Human and mouse islets were gently dispersed, loaded with 1 μM Fura-4F-AM for single-cell Ca^{2+} imaging studies as described (1, 16). Ringer's solutions contained 3 mM glucose, unless otherwise indicated.

Calpain Expression and Activity—Calpain mRNA was measured semi-quantitatively in 50 islets using reverse transcriptase-PCR with GAPDH and β-actin as internal standards, as described (1). Calpain activity was measured in intact mouse islets loaded with the fluorogenic

* This work was supported by National Institutes of Health Grants P60 DK-20579, DK-31842 (to K. S. P.), DK-20595 and DK-47486 (to G. I. B.), and the Kovler Foundation. The costs of publication of this article were defrayed in part by the payment of page charges. This article must therefore be hereby marked "*advertisement*" in accordance with 18 U.S.C. Section 1734 solely to indicate this fact.

§ Supported by fellowships from the Natural Sciences and Engineering Research Council of Canada, the Canadian Institutes of Health Research, and the Juvenile Diabetes Research Foundation.

‡‡ To whom correspondence should be addressed. E-mail: polonsky@im.wustl.edu.

[1] The abbreviations used are: ER, endoplasmic reticulum; IP_3, inositol trisphosphate; RyR, ryanodine receptor; DEVD-CHO, Asp-Glu-Val-Asp/Chinese hamster ovary; TUNEL, terminal deoxynucleotidyltransferase-mediated dUTP nick end labeling; ES, embryonic stem; ALLM, *N*-acetyl-Leu-Leu-Met-CHO; CICR, Ca^{2+}-induced Ca^{2+} release.

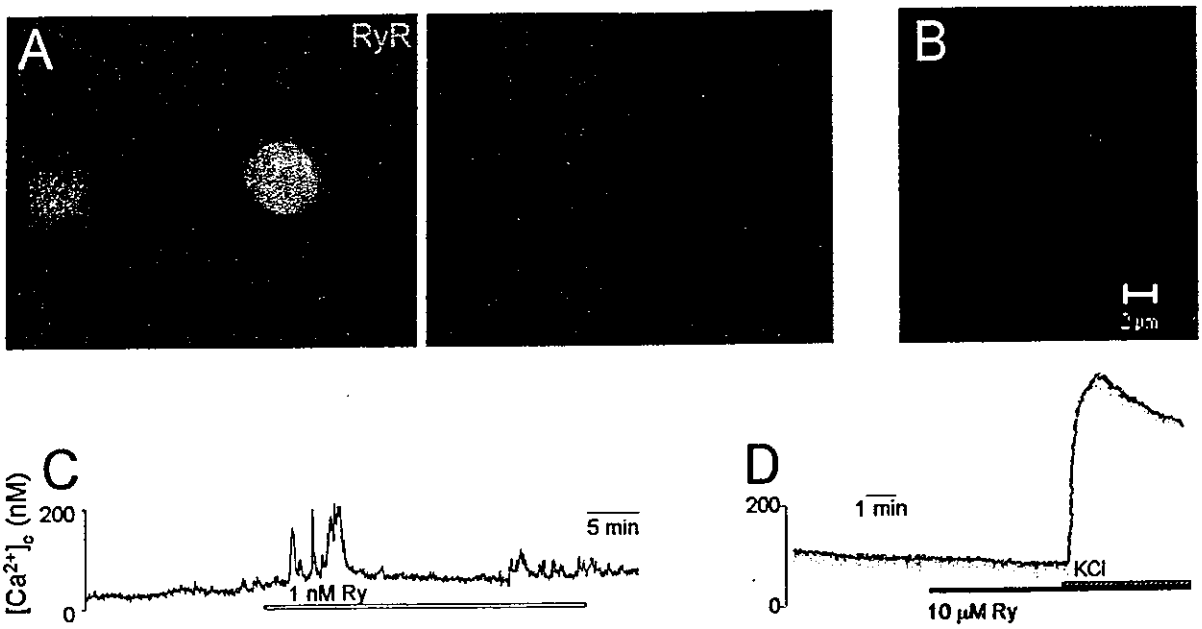

FIG. 1. **Localization of RyR in β-cells.** *A*, double-immunofluorescence staining of dispersed human islet cells for RyR (*left panel*) and for insulin (*right panel*). Approximately 80% of β-cells expressed RyR. RyR was also expressed in non-β-cells. Similar results were seen in cultures of primary mouse β-cells. No staining was seen when primary antibody was excluded. *B*, confocal microscopy of mouse β-cells showed a vesicular distribution of RyR. *C*, 1 nM ryanodine induced an increase in cytosolic Ca^{2+} in single β-cells. *D*, no increase in cytosolic Ca^{2+} was seen in unstimulated cells exposed to 10 μM ryanodine (or 100 μM ryanodine, not shown). 30 mM KCl was used as a positive control. The average $[Ca^{2+}]_c$ trace of 25 cells is shown with hanging S.E. bars. Ca^{2+} imaging experiments are representative of at least three independent experiments in both human and mouse cell cultures.

calpain substrate, Boc-Leu-3-O-[3H]methyl-D-Met-CMAC [10 mmol/liter], as described previously (25, 26). Calpain activity was quantified by using the initial slope (0–10 min).

Measurement of Apoptosis—We used four independent methods to measure apoptosis in primary islets and MIN6 cells: namely, PCR-enhanced DNA laddering, ApoPercentage dye labelling, cell density/viability, and terminal deoxynucleotidyltransferase-mediated dUTP nick end labeling (TUNEL). The PCR-enhanced DNA ladder analysis was adapted from the ApoAlert Kit (Clontech, Palo Alto, CA) to measure apoptosis in groups of 8–15 islets. This method is semi-quantitative and extremely sensitive (*i.e.* requires very little tissue). This approach uses adapter nucleotides and short PCR runs to selectively amplify DNA ladders. Briefly, after lysing islets at 55 °C for 15 min, genomic DNA was isolated by using the DNeasy kit (Qiagen, Valencia, CA), taking great care not to break the large strands of DNA; concentration was quantified by UV spectrophotometry. 200 ng of genomic DNA was ligated to adapters using T4 ligase (New England Biolabs, Beverly, MA) at room temperature for 2 h. PCR products were run on a 2% agarose/ethidium bromide gel in 0.5× TBE (90 mM Tris/64.6 mM boric acid/2.5 mM EDTA, pH 8.3). DNA ladders were quantified as the mean intensity using Adobe Photoshop. This approach is conservative because blank lanes exhibit a small amount of gray-scale density. For each gel, DNA ladder density was expressed as a percentage of untreated/wild-type islets. These percentages were then averaged to give the mean change ± S.E. for each condition.

Apoptosis in single isolated human or mouse islet cells was examined qualitatively using the ApoPercentage dye (Biocolor, Belfast, Northern Ireland), as described previously (1). This dye labels live cells bright pink that are undergoing phosphatidylserine translocation to the outer plasma membrane, a characteristic of apoptosis, but not necrosis. Non-apoptotic cells remain clear.

Cell death was measured quantitatively in cultures of MIN6 cells by measuring viability/cell density and by TUNEL analysis using the DeadEnd Colorimetric kit (Promega, Madison, WI) as described (1). The number of cells in each well and the number of TUNEL-positive cells were quantified using MetaMorph™ image analysis software. To further characterize MIN6 cell apoptosis, cells were stained with antibody recognizing the active, cleaved form of caspase-3 (Trevigen Inc., Gaithersburg, MD).

β-Cell-specific Calpastatin and Calpain-10 Transgenic Mice—Animal use protocols were approved by Washington University. Male mice, 8–30 weeks old, and littermate controls were used for all experiments. Transgenic mice were engineered by standard techniques. The rat insulin 2 promoter was used to drive the expression of human calpastatin or human calpain-10a using the strategies outlined (see Figs. 4 and 7). The expression of the human calpastatin transgene was confirmed by immunohistochemistry of pancreatic sections as described previously (1) using an antibody to human calpastatin (Calbiochem). The expression of the human calpain-10a transgene was confirmed by immunoblot using a polyclonal calpain-10 antibody from Biogenesis (Kingston, NH). The function of the transgenes was confirmed using measurements of islet calpain activity.

Calpain-10 Knockout Mice—Calpain-10 knockout mice ($Capn10^{-/-}$) were generated by deleting exon 2, as follows. A BAC clone containing *Capn10* from a 129/SvJ mouse genomic library (Genome Systems Inc, St. Louis, MO). A BamHI/SpeI (6.9 kb) fragment was used to construct a gene-targeting vector pACN-Capn10. A self-excision ACN cassette was inserted at a BglII site (5′ of exon 2) and loxP sequence at an *Sna*BI site (3′ of exon 2). A targeting vector was designed to delete the predicted active-site Cys^{73} in exon 2 of the gene. Linearized pACN-Capn10 plasmid was electroporated into embryonic stem (ES) cells. Genomic DNA from G418-resistant ES cell clones was analyzed for homologous recombination by Southern blotting. Two ES cell clones containing the targeted mutation were injected into C57BL/6B embryos. Chimeric mice were backcrossed to C57BL/6B mice. Germline transmission of the mutant allele was detected by Southern blot and PCR analysis of tail DNA from F1 offspring with Agouti coat color. One ES clone showed germline transmission. Homozygous $Capn10^{-/-}$ mice from the F1 cross were identified by PCR. The recombinant $Capn10^{ACN}$ allele was also confirmed by Southern blotting (not shown). The loss of calpain-10 protein expression was confirmed by Western blotting of brain lysates using an affinity-purified anti-calpain-10 antibody generated against a 15 amino acid peptide of human calpain-10 (^{194}GGQQDRPGRWEHRTC^{208}) from Research Genetics (Huntsville, AL).

Statistical Analysis—The unpaired *t* test was used to test the significance of differences between groups. Differences were considered significant when $p < 0.05$. Results are presented as mean ± S.E.

RESULTS

Localization of Active RyR in Human and Mouse β-Cells—Immunofluorescence staining demonstrated the presence of RyR in a majority of human and mouse β-cells (Fig. 1*A*). Confocal studies of RyR localization showed a punctate and vesicular pattern of expression (Fig. 1*B*). Although previous studies have documented the presence of specific ryanodine-binding

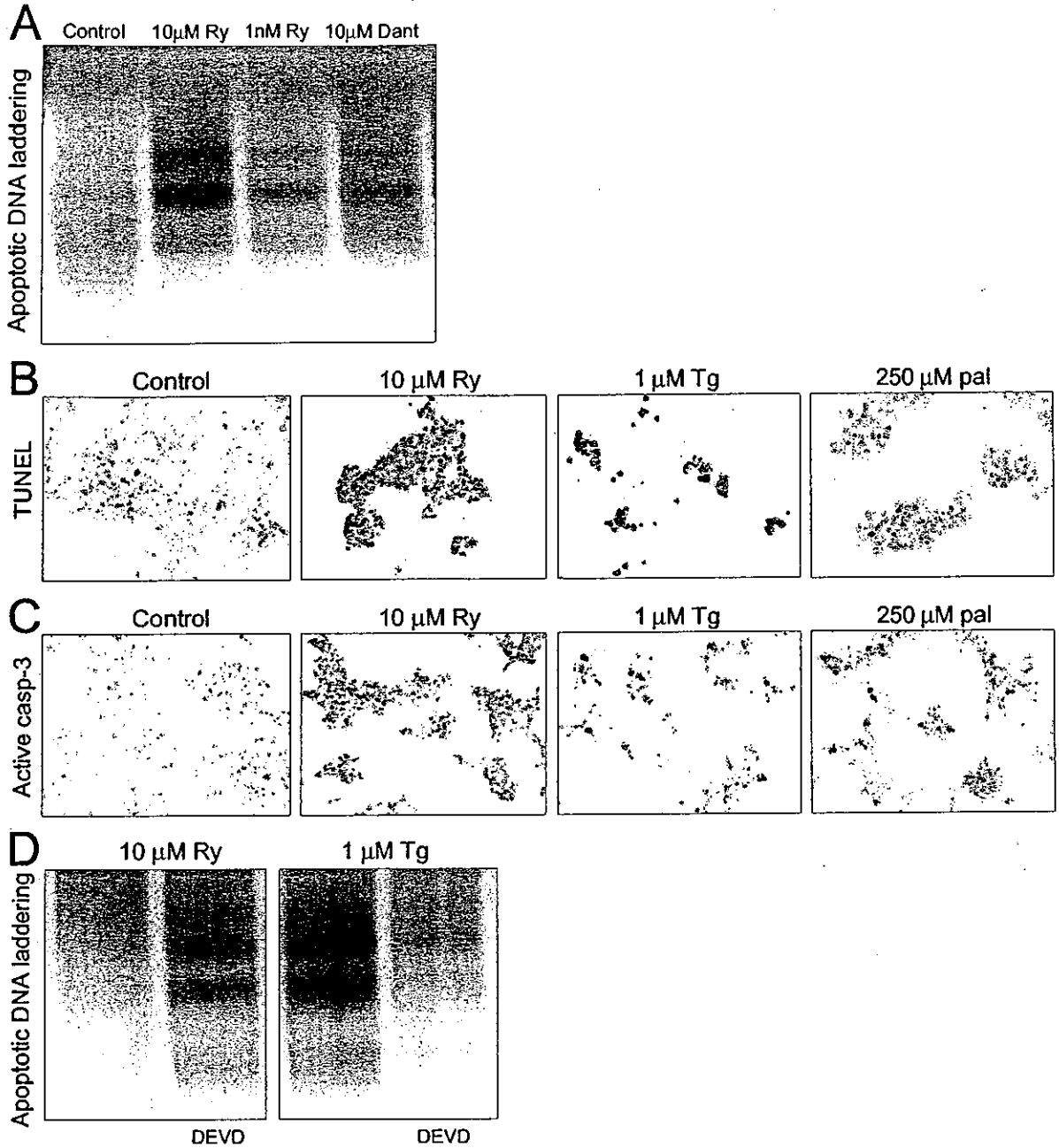

FIG. 2. **Inhibiting RyR2 induces apoptosis in human and mouse islets that is not caspase-3-dependent.** *A*, DNA laddering was significantly greater than control in human islets cultured for 36 h in 10 μM ryanodine (232 ± 33% *versus* control, $p < 0.05$), but not 1 nM ryanodine (109 ± 6% *versus* control) or 10 μM dantrolene (115 ± 16% *versus* control) ($n = 4$). The average intensity (±S.E.) of the DNA ladders is indicated as a percentage of control islets. *B*, cell density analysis of MIN6 cells demonstrated a significant loss of cells in cultures treated with 10 μM ryanodine (71 ± 2% *versus* control, $p < 0.05$), 1 μM thapsigargin (44 ± 1% *versus* control, $p < 0.05$) or 250 μM palmitate (93 ± 3% *versus* control, $p < 0.05$; $n = 3$). A significant increase in *red* TUNEL-positive cell nuclei is also seen in these representative images. *C*, normalized to control, the percentage of active caspase-3-positive MIN6 cells (stained *red*), relative to the total number of cells in each treatment, was 129 ± 7% for ryanodine ($p < 0.05$), 1679 ± 15% for thapsigargin ($p < 0.05$), and 232 ± 3% for palmitate ($p < 0.05$; $n = 3$). *D*, in ryanodine-treated mouse islets, the caspase-3 inhibitor DEVD-CHO (10 μM) did not block apoptosis (123 ± 22%; $n = 3$). DEVD-CHO reduced apoptosis 69 ± 11% ($p < 0.05$) in mouse islets treated with 1 μM thapsigargin) ($n = 3$).

sites and mRNA for RyR2 in human and rodent β-cells (17, 22), whether these Ca^{2+} channels are functional has not been directly tested. Nanomolar concentrations of ryanodine, which bind to the open RyR channel pore and increase the probability that the channel will open (27, 28), evoked an increase in cytosolic Ca^{2+} in β-cells from mouse islets (Fig. 1*C*) and human islets (18). This finding suggests that β-cell RyR are active under basal conditions. Micromolar concentrations of ryanodine, which inhibit the RyR, did not elevate cytosolic Ca^{2+} in unstimulated cells (Fig. 1*D*). These findings provide strong evidence that functional RyR are present in both human and mouse β-cells.

Role of RyR in β-Cell Apoptosis—We employed several approaches to determine whether ryanodine induced apoptosis in cultured islets, including PCR-enhanced DNA ladder analysis, a sensitive technique for detecting DNA fragments generated during apoptosis but not necrosis (1). DNA ladders, reflecting the organized cleavage of DNA, were detected within 36 h after exposure of human islets (Fig. 2*A*) or mouse islets (see below) to a blocking concentration (10 μM) of ryanodine. In contrast,

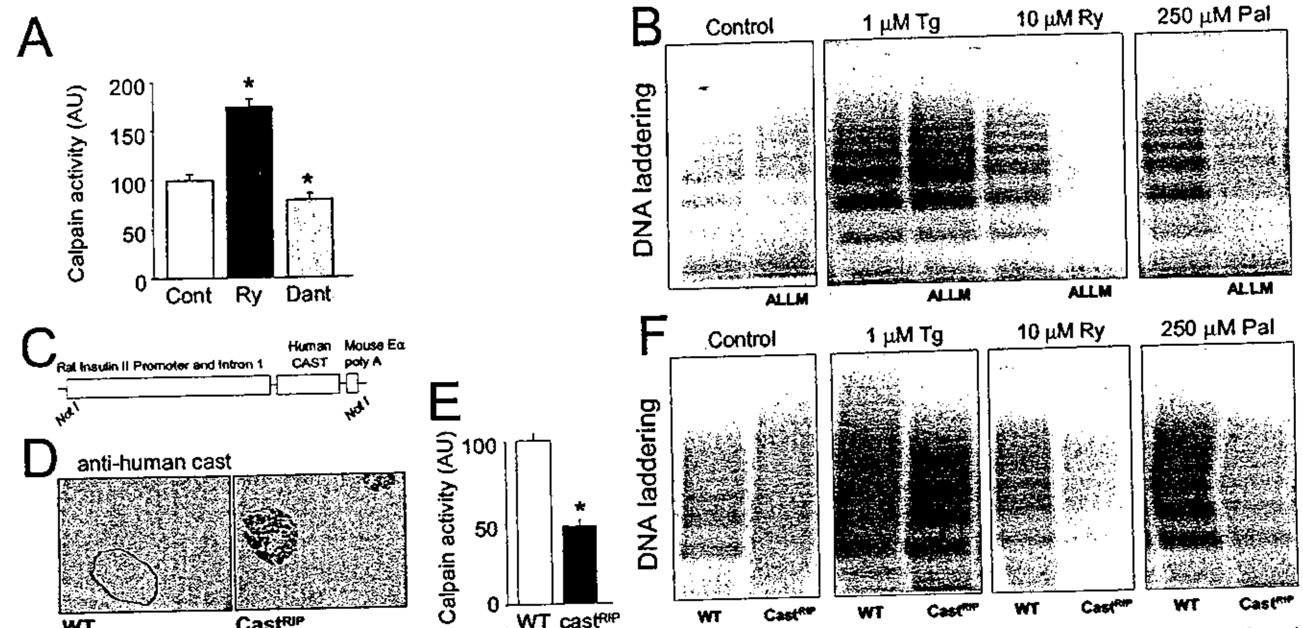

FIG. 3. **Ryanodine-induced apoptosis is mediated by calpain activation.** *A*, 36-h culture with ryanodine (n = 12), but not dantrolene (n = 8), increased calpain activity over control (n = 8). *B*, effect of the calpain inhibitor ALLM on apoptosis under 10 mM glucose basal conditions (103 ± 22% *versus* no ALLM) and apoptosis induced by 60-h culture with 1 μM thapsigargin (98 ± 6% *versus* no ALLM), 10 μM ryanodine (49 ± 12% *versus* no ALLM, p < 0.05) or 250 μM palmitate (72 ± 7% *versus* no ALLM, p < 0.05; n = 4–6). *C*, transgene construct for mice that over-express calpastatin in β-cells (Cast^{RIP}). *D*, representative immunohistochemical staining using an antibody to human calpastatin in paraffin-embedded pancreas sections from wild-type (*left panel*) and Cast^{RIP} mice (*right panel*). No staining is seen in an islet (*left panel, blue outline*) from wild-type mice. *E*, reduced calpain activity in islets isolated from Cast^{RIP} mice. *Asterisks* denote significant difference (p < 0.05) from control. *F*, apoptosis in islets from Cast^{RIP} mice was compared after 60-h culture in 10 mM glucose control conditions (95 ± 11% *versus* wild type), 1 μM thapsigargin (102 ± 5% *versus* wild type), 10 μM ryanodine (55 ± 1% *versus* wild type, p < 0.05) or 250 μM palmitate (65 ± 8% *versus* wild type, p < 0.05) (n = 8).

activation of RyR with 1 nM ryanodine or inhibition of RyR1 with dantrolene did not induce significant apoptosis. We confirmed that 10 μM ryanodine induced apoptosis by measuring phosphatidylserine translocation in human β-cells (not shown), as well as by measuring a decrease in cell number and an increase in TUNEL-positive cells in the MIN6 cell line (Fig. 2*B*). Together, these results indicate that inhibition of basal Ca^{2+} flux through RyR2 activates β-cell apoptosis.

The Role of Caspase-3 in Ryanodine-induced Apoptosis—The mechanism of ryanodine-induced apoptosis was studied in comparison with two known inducers of β-cell apoptosis, thapsigargin and the free fatty acid palmitate (1, 8). The mechanism of the potent effect of palmitate on apoptosis is poorly understood. Thapsigargin causes ER stress and induces apoptosis by depleting IP_3-sensitive Ca^{2+} stores that are distinct from those targeted by ryanodine in β-cells (29). In contrast to thapsigargin-induced apoptosis (9), apoptosis caused by inhibiting RyR2 was associated with relatively little caspase-3 activation (Fig. 2*C*). Apoptosis induced by palmitate showed an intermediate association with caspase-3 activation, when compared with ryanodine and thapsigargin. To address whether ryanodine-induced cell death was mediated by caspase-3, we treated islets with the membrane permeant caspase-3 inhibitor DEVD-CHO. Ryanodine-induced apoptosis was not inhibited by DEVD-CHO, whereas thapsigargin-induced apoptosis was significantly reduced (Fig. 2*D*). The implication of a cell death pathway relatively independent of caspase-3 prompted us to test whether an alternate pathway, involving calpain, mediated β-cell apoptosis in response to ryanodine.

Role of the Calpain System in β-Cell Apoptosis—Ryanodine, but not dantrolene, increased calpain activity in mouse islets (Fig. 3*A*). The small molecule calpain inhibitor *N*-acetyl-Leu-Leu-Met-CHO (ALLM), which we have previously shown decreases calpain activity by >50% in islets (25), blocked ryanodine-induced apoptosis but had no effect on thapsigargin-induced apoptosis or basal apoptosis (Fig. 3*B*). ALLM also

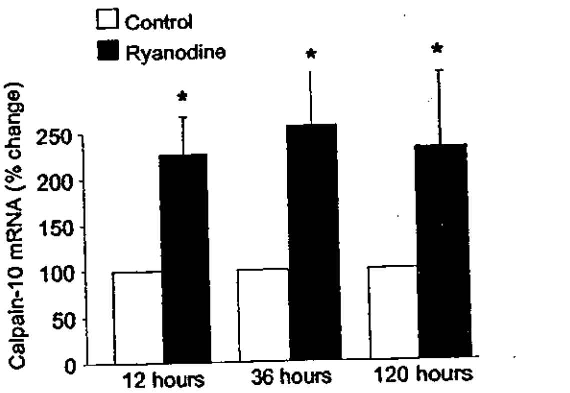

FIG. 4. **Ryanodine specifically induces calpain-10 gene expression.** *A*, calpain-10 mRNA was increased after 12-, 36-, and 120-h treatment with 10 μM ryanodine, as assessed with RT-PCR. The band intensity of the calpain-10 PCR product was normalized to that of GAPDH. Calpain-10 mRNA levels from islets treated with ryanodine are expressed as a percentage of untreated cells. Similar results were seen by using real-time PCR (not shown). *Asterisks* denote significant difference (p < 0.05) from control.

blocked apoptosis induced by palmitate. A genetic approach was used to confirm the role of calpain in β-cell apoptosis. We generated transgenic mice that express calpastatin, an endogenous calpain inhibitor protein (30), exclusively in β-cells using the rat insulin promoter (Cast^{RIP} mice; Fig. 3*C*). Calpain activity was reduced more than 50% in islets from these mice (Fig. 3*E*), and this was associated with reductions in apoptosis induced by ryanodine or palmitate (Fig. 3*F*). The reduction in β-cell apoptosis with ALLM and calpastatin, both of which inhibit multiple isoforms of calpain, establishes an important role for a calpain-mediated pathway in this process.

The Role of Calpain-10 in β-Cell Apoptosis—Next, we sought to determine the specific isoform of calpain that is involved in ryanodine- and palmitate-induced apoptosis. Ry-

anodine increased calpain-10 mRNA in mouse islets by ~2.5-fold (Fig. 4, confirmed by real-time PCR, not shown), but had no significant effect upon calpain 1 and calpain 2 mRNA (not shown). Importantly, the ryanodine-induced increase in mRNA was an early event, evident by 12 h and lasting at least 5 days. To define the role of calpain-10 in β-cell apoptosis, we examined Capn10$^{-/-}$ islets from mice in which the calpain-10 gene had been deleted (Fig. 5*A*). Ryanodine failed to increase calpain activity in Capn10$^{-/-}$ islets (Fig. 5*B*). Ryanodine-induced apoptosis and palmitate-induced apoptosis were also prevented in Capn10$^{-/-}$ islets (Fig. 5*C*). Conversely, ryanodine-induced apoptosis was enhanced in islets from transgenic mice with β-cell-specific overexpression of human calpain-10 (Fig. 6, *A–C*, *Capn10^{RIP}*). Capn10^{RIP} islets showed enhanced calpain activity (Fig. 6*D*), suggesting that our assay measures the activity of calpain-10, in addition to other calpains. Together, the results strongly suggest that calpain-10 mediates apoptosis induced by inhibition of RyR2. The observation that apoptosis resulting from exposure to palmitate was inhibited in Capn10$^{-/-}$ islets and enhanced in Capn10^{RIP} islets suggests that cell death induced by free fatty acids shares common steps with the RyR2 pathway.

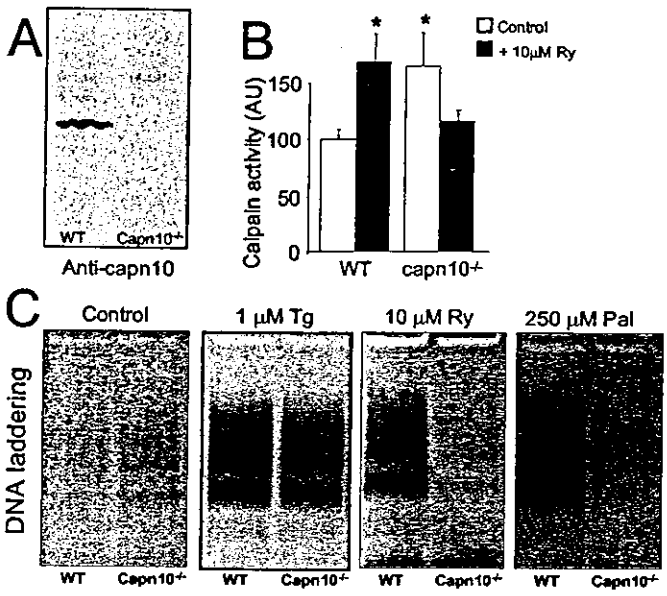

FIG. 5. **Calpain-10 is required for ryanodine- and palmitate-induced apoptosis.** *A*, a fragment of ~25 kDa was apparent in immunoblot of brain lysate from wild type but not Capn10$^{-/-}$ mice. *B*, calpain activity after 36-h culture was measured in the presence or absence of 10 μM ryanodine in wild-type or Capn10$^{-/-}$ islets. *Asterisks* denote significant difference ($p < 0.05$) from control. *C*, apoptosis in islets from Capn10$^{-/-}$ mice was compared after 60-h culture in 10 mM glucose control conditions (100 ± 9% *versus* wild type), 1 μM thapsigargin (72 ± 15% *versus* wild type), 10 μM ryanodine (51 ± 6% *versus* wild type, $p < 0.05$) or 250 μM palmitate (56 ± 9% *versus* wild type, $p < 0.05$) ($n = 6$).

Effects of GLP-1 on Calpain Activity and Apoptosis—We next tested whether agents known to promote β-cell survival may act by modulating the RyR2/calpain-10 pathway. GLP-1, a potent inhibitor of β-cell apoptosis (31), mobilizes intracellular Ca^{2+} and activates mitochondria via RyR (17, 20). GLP-1 decreased basal calpain activity and abolished ryanodine-induced calpain activation (Fig. 7*A*). GLP-1 also prevented apoptosis and cell loss in MIN6 cells treated with ryanodine (Fig. 7*B*). Similar results were seen with the GLP-1 receptor agonist, exendin-4 (not shown). Thus, the anti-apoptotic effects of GLP-1 may, in part, be due to activation of RyR2 and subsequent inhibition of calpain activity.

Interaction between Glucose and RyR2—The glucose level to which pancreatic islets are exposed is another important determinant of apoptosis (1, 4–6, 32). First, we wanted to determine the relationship between glucose signaling and RyR2. Surprisingly, ryanodine had significant effects on Ca^{2+} homeostasis during stimulation with glucose or KCl, in contrast to the situation in the basal conditions (3 mM glucose) described in Fig. 1. Concentrations of ryanodine that inhibit RyR potentiated the Ca^{2+} response to elevated glucose in a subpopulation of human or mouse β-cells (Fig. 8, *A* and *B*) and Ca^{2+} responses to 30 mM KCl in all cells (Fig. 8*C*), suggesting that ryanodine-sensitive

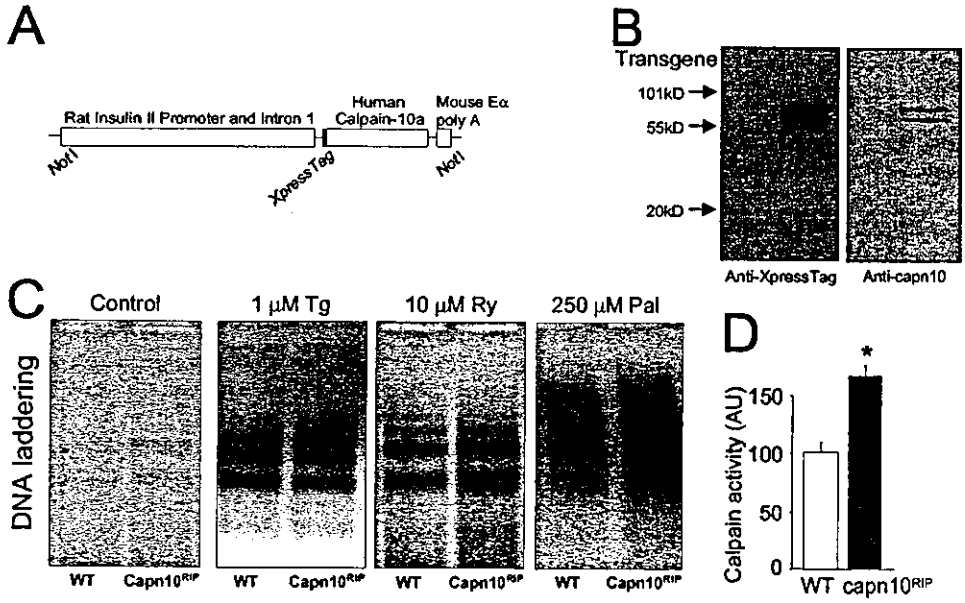

FIG. 6. **Transgenic over-expression of calpain 10 enhances ryanodine- and palmitate-induced apoptosis.** *A*, transgene construct for Capn10^{RIP} mice. *B*, Western blot of islet lysate using antibodies for the Xpress Tag (*right panel*) and an antibody to human calpain 10 (Biogenesis, *left panel*). The band below ~94 kDa is abundant in transgenic tissue and is approximately the expected size of calpain-10 (including the Xpress tag). *C*, apoptosis in islets from Capn10^{RIP} mice was compared after 60-h culture in 10 mM glucose control conditions (117 ± 22% *versus* wild type), 1 μM thapsigargin (114 ± 16% *versus* wild type), 10 μM ryanodine (138 ± 11% *versus* wild type, $p < 0.05$) or 250 μM palmitate (125 ± 10% *versus* wild type, $p < 0.05$) ($n = 6$). *D*, calpain activity is increased in islets from Capn10^{RIP} mice. *Asterisks* denote significant difference ($p < 0.05$) from control.

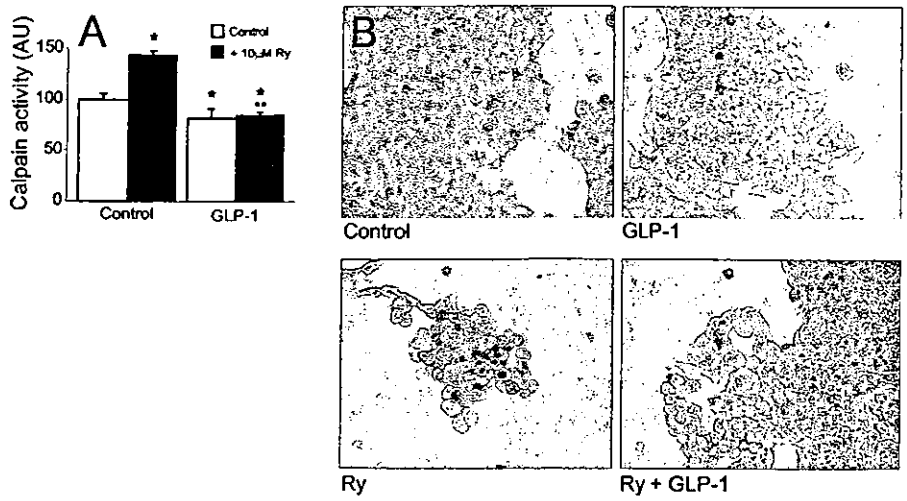

FIG. 7. **GLP-1 inhibits calpain activity and protects β-cells from ryanodine-stimulated apoptosis.** *A*, 100 nM GLP-1 blocked ryanodine-stimulated calpain activity in 36-h cultures (n = 8–11). *, significant difference from control; **, significant difference from ryanodine-treated islets. *B*, cell density and TUNEL (*red* nuclei) analysis of MIN6 cells treated with 10 μM ryanodine (*bottom panels*) in the presence (*right panels*) or absence (*left panels*) of GLP-1 (100 nM). Ryanodine induced significant cell loss and a robust increase in TUNEL-positive MIN6 cells. The effects of ryanodine were blocked in MIN6 cells treated with GLP-1, which showed similar levels of cell density and TUNEL staining when compared with control or cells treated with GLP-1 alone.

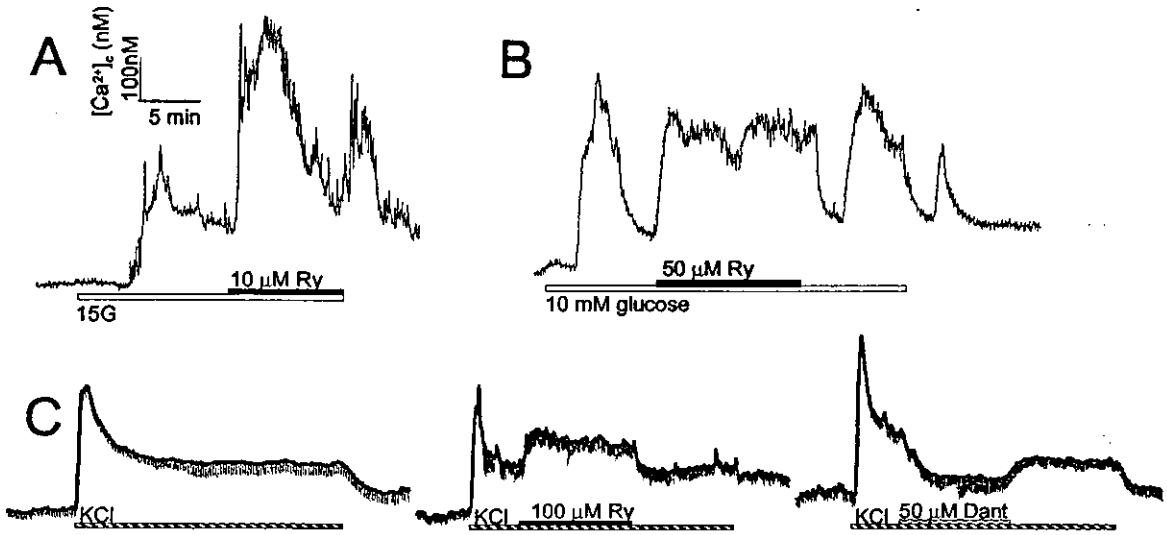

FIG. 8. **RyR2 are involved in buffering Ca^{2+} influx during β-cell stimulation with glucose or KCl.** *A*, 10 μM ryanodine further increased cytosolic Ca^{2+} in 20% of dispersed human β-cells responding to 15 mM glucose. *B*, 50 μM ryanodine also potentiated 10 mM glucose-evoked Ca^{2+} signals in mouse β-cell. Because of the variable pattern of responses to glucose, representative traces are shown. Similar results were seen in dispersed mouse β-cells (not shown). *C*, the increase in cytosolic Ca^{2+} in human β-cells evoked by 30 mM KCl is further enhanced by 100 μM ryanodine. Blocking RyR1 with dantrolene (50 μM) reduced KCl-induced Ca^{2+} levels. Average traces with hanging S.E. bars are shown. All traces are on the same scale.

Ca^{2+} stores are involved in Ca^{2+} uptake under these conditions. In contrast, dantrolene evoked an immediate decrease in Ca^{2+} in stimulated β-cells, consistent with a role for RyR1 in Ca^{2+}-induced Ca^{2+} release (CICR). Neither stimulating RyR with 1 nM ryanodine nor blocking IP_3R with xestospongin C had any effect upon depolarization-induced Ca^{2+} responses (18). These findings suggest that RyR2 play a novel non-CICR role during glucose-induced Ca^{2+}-influx, whereas RyR1 mediates CICR in β-cells. Having established the link between glucose signaling and RyR2, we examined whether high glucose modulates calpain activity and protects islets from ryanodine-induced apoptosis, because short-term exposure (*i.e.* 2 days) to high glucose (25 mM) has been shown to inhibit β-cell apoptosis (33). This experiment would also shed some light on the possible mechanisms of ryanodine-induced apoptosis. Notably, if 10 μM ryanodine were causing apoptosis by augmenting CICR, 25 mM glucose would be expected to potentiate ryanodine-induced cell death. However, a 2-day culture of islets in 25 mM glucose blocked ryanodine-stimulated calpain activity and ryanodine-induced apoptosis (Fig. 9). Thus, the beneficial effects of short-term exposure to high glucose on β-cell survival may be mediated by a novel interaction with RyR2. Accordingly, we also examined the role of the RyR2/calpain pathway in cell death caused by a lowered rate of β-cell metabolism. Apoptosis induced by *in vitro* hypoglycemia (2 mM glucose for 60 h) was completely absent in Capn10$^{-/-}$ islets (Fig. 10*A*). On the other hand, apoptosis was enhanced in Capn10^{RIP} islets incubated in moderately low glucose (5 mM) but not at 10 mM or 25 mM glucose (Fig. 10*B*). These results suggest that calpain-10 plays an important role in apoptosis induced by exposure to low glucose concentrations but not apoptosis induced by prolonged exposure to high glucose concentrations. Thus, the RyR2/calpain-10 death pathway is turned on when β-cell metabolic activity is low and turned off by stimuli that increase metabolic activity.

Roles of RyR2 and Calpain-10 in Apoptosis Induced by Chronic Hyperglycemia—Unlike the pro-survival effects of short incubations in 25 mM glucose, chronic stimulation (*i.e.* 7 days) with high glucose induces apoptosis (1, 32). Apoptosis induced by chronic (7 day) hyperglycemia was not affected by calpain-10 knockout (Fig. 10*C*) or calpastatin over-expression (102 ± 15% *versus* wt, n = 6), suggesting that apoptosis mediated by high glucose does not involve a calpain-10-dependent pathway. Like thapsigargin-induced apoptosis, glucose toxicity is known to involve caspase-3 (32). Therefore, the RyR2/calpain-10 apoptosis pathway is separate from other known β-cell apoptosis pathways.

Interestingly, inhibiting RyR protected β-cells against apoptosis induced by 7-day culture in high glucose (Fig. 10*D*). Therefore, we tested whether the protective effect of ryanodine on apoptosis induced by chronic stimulation may be mediated by blocking CICR through RyR1. Apoptosis induced by chronic exposure to high glucose was inhibited by dantrolene (Fig. 10*E*), implicating RyR1 and CICR in this process. A prominent role for dantrolene-sensitive RyR in excitotoxic neuronal cell death has been proposed (34).

DISCUSSION

The present studies were undertaken to assess the role of RyR in the survival of pancreatic β-cells and to determine the mechanism by which these Ca^{2+} channels regulate apoptosis. Our findings indicate that inhibiting the RyR2 is associated with increased apoptosis, suggesting that maintenance of normal basal Ca^{2+} flux through this channel is essential for β-cell survival. To our knowledge, these are the first results in any cell type to suggest that blocking RyR can induce apoptosis, although excessive RyR activity has been linked to cell death in other tissues, including the brain and heart (30, 35). That RyR2 may be a central molecule in the control of programmed cell death is perhaps not surprising. RyR are very large proteins that can directly sense cytosolic Ca^{2+}, luminal Ca^{2+}, ATP, redox potential, and nitric oxide (36), thus placing them in a key position to integrate multiple signals known to influence apoptosis. The general importance of RyR2 activity is underscored by the embryonic lethality of $RyR2^{-/-}$ mice after embryonic day 9.5 (37). In contrast, no differences in islet morphology or β-cell ultrastructure were observed in mice lacking both RyR1 and RyR3 (38). Previous studies have reported that the expression of RyR2 is reduced in islets from several rodent models of diabetes (22). Together, these results suggest that RyR2 may be important in apoptosis in the β-cell and could, therefore, be involved in the impairment of insulin secretion and the pathogenesis of diabetes.

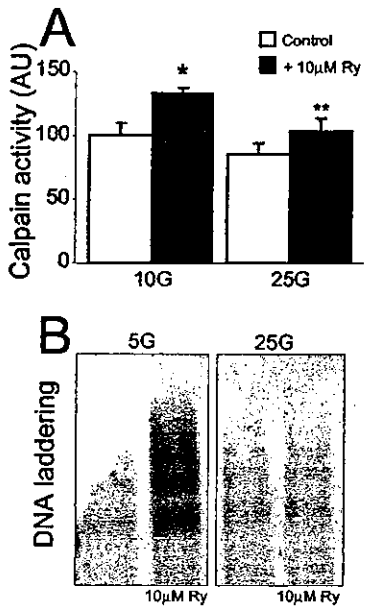

FIG. 9. **Effects of short-term treatment with high glucose on ryanodine-induced calpain activity and apoptosis.** *A*, ryanodine-stimulated calpain activity was significantly lower after a 60-h incubation in 25 mM glucose, compared with 10 mM glucose. *, significant difference from control; **, significant difference from ryanodine-treated islets. *B*, although ryanodine induced significant apoptosis in mouse islet culture for 48 h in 5 mM glucose (200 ± 14% *versus* no ryanodine, $p < 0.05$), no additional apoptosis was seen in 25 mM glucose (96 ± 3% *versus* no ryanodine).

Our results define a number of novel aspects of the mechanisms of apoptosis in the pancreatic β-cell. We have clearly demonstrated the existence of multiple pathways leading to β-cell apoptosis (Fig. 11). In the pancreatic β-cell, as least two major two apoptosis pathways are apparent, based upon their requirement for calpain-10 or caspase-3. Thapsigargin-induced ER stress and chronic hyperglycemia are known to be associated with the classical caspase-3-dependent pathway (5, 9). On the other hand, a novel calpain-10-dependent apoptosis pathway mediates cell death induced by ryanodine, hypoglycemia, and palmitate. Whether the pathways associated with these apoptotic stimuli involved additional molecules other than calpain-10 remains to be determined. Although we present evidence that RyR2 participates in glucose-induced Ca^{2+} signaling, the link between RyR2 and palmitate remains unclear. Although other calpain isoforms have been suggested to regulate cell death in other tissues, our results are the first to demonstrate that any calpain isoform is involved in apoptosis in primary β-cells. Previously, we have shown that prolonged

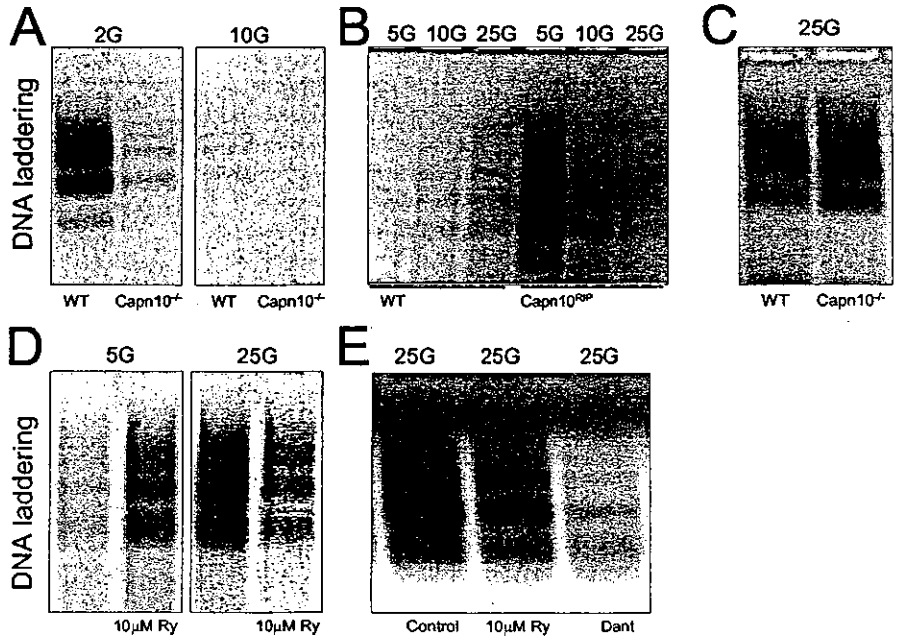

FIG. 10. **Calpain-10 mediates apoptosis induced by exposure to low glucose.** *A*, the increase in apoptosis induced by 2 mM glucose was prevented in $Capn10^{-/-}$ islets, (51 ± 11% *versus* wild type, $p < 0.05$), but was not different under basal conditions (101 ± 9% *versus* wild type) ($n = 3$). *B*, after 60 h, $Capn10^{RIP}$ islets demonstrated enhanced apoptosis in 5 mM glucose (289 ± 53% *versus* wild type, $p < 0.05$), but not in 10 mM glucose (117 ± 22% *versus* wild type) or 25 mM glucose (110 ± 7% *versus* wild type) ($n = 3$). *C*, apoptosis induced by 7-day exposure to 25 mM glucose is not reduced in islets from $Capn10^{-/-}$ mice (107 ± 9% *versus* wild type) ($n = 6$). *D*, in mouse islets cultured for 7 days, 10 μM ryanodine increased apoptosis in 5 mM glucose (144 ± 19% *versus* no ryanodine, $p < 0.05$), but reduced apoptosis in 25 mM glucose (70 ± 9% *versus* no ryanodine, $p < 0.05$) ($n = 4$). *E*, apoptosis was reduced in human islets stimulated for 7 days with 25 mM glucose when treated with 10 μM ryanodine (80 ± 6% *versus* untreated, $p < 0.05$) or 10 μM dantrolene (74 ± 11% *versus* untreated, $p < 0.05$) ($n = 3$).

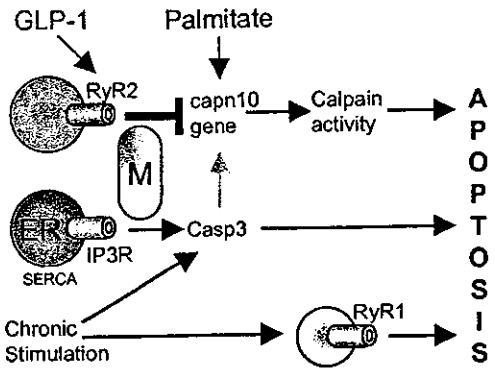

FIG. 11. **Proposed model of the RyR2/calpain 10 life/death pathway in β-cells.** Ca^{2+} flux through RyR2 normally suppresses calpain-10 gene expression and activity. RyR2-containing Ca^{2+} stores can be activated by acute glucose treatment or GLP-1 and are closely associated with mitochondria (*M*). Palmitate-induced apoptosis also requires calpain-10. ER-stress of thapsigargin/IP_3-sensitive Ca^{2+} stores leads to apoptosis largely mediated by caspase-3 activation, although some cross-talk between the caspase-3 pathway and the calpain-10 pathway may occur. Chronic stimulation by high glucose also utilizes calpain-10-independent pathways, including possible CICR by means of RyR1-like signaling.

incubation with calpain inhibitors has deleterious effects upon the function of mouse islets (26). However, the links between inhibition of RyR2 activity, increased calpain-10 expression, and apoptosis have not been identified previously. Genetic variation in the calpain-10 gene has been linked to increased susceptibility to diabetes (39), although the function of the calpain-10 protein was not known.

We have shown that the RyR2/calpain-10 pathway can be directly modulated by high glucose and GLP-1. Both treatments would be expected to stimulate mitochondrial activity, and both are known to protect β-cells from apoptosis (20, 31, 33). In addition, GLP-1 signaling in human β-cells and MIN6 cells is known to be mediated by RyR-gated intracellular Ca^{2+} stores (17, 20). Our results suggest that the stimulation of Ca^{2+} release from RyR2, possibly leading to increased mitochondrial ATP production (20), and the suppression of calpain activity may be important mechanisms by which GLP-1 promotes β-cell survival. GLP-1, or related agonists that activate RyR2, may be useful, therefore, in the context of clinical islet transplantation, where apoptosis during the procurement, isolation, storage, and engraftment of islets is a significant problem. Because improved hematopoietic stem cell engraftment was seen with exposure to cyclic ADP ribose (40), an endogenous activator of RyR2, the possibility that this pathway could be modulated to improve graft survival in human islet transplantation should be examined. Interestingly, we have documented distinct effects of RyR1 and RyR2 on apoptosis. Under basal conditions, Ca^{2+} flux through RyR2 is required to prevent apoptosis, whereas active RyR1 are critical for the deleterious effects of prolonged stimulation with high glucose, consistent with a CICR mechanism. These studies, therefore, suggest that both the RyR1 and RyR2 should be explored as novel targets for diabetes drug development. Although multiple studies in other endocrine cell types have made use of the specificity of ryanodine for the RyR (41–43), and we are not aware of alternate molecular targets of this agent (23, 24), the molecular ablation of RyR2 will be required to confirm our findings.

In conclusion, our results are the first to clearly define a physiological role in any tissue for calpain-10, recently identified as a type 2 diabetes susceptibility gene by linkage studies and positional cloning (39). The demonstration that a RyR2/calpain-10 pathway plays a critical role in β-cell survival suggests novel mechanisms for the pathophysiology of β-cell dysfunction in type 2 diabetes as well as novel targets for therapeutic intervention to preserve β-cell function. Our results may also provide a new framework for the investigation of potential mechanisms whereby alterations in Ca^{2+} handling by RyR may lead to cell death in other pathological states, such as Alzheimer's disease, ischemia/reperfusion injury, and heart failure.

Acknowledgments—We thank the Juvenile Diabetes Research Foundation Human Islet Isolation Core and the Diabetes Research and Training Center at Washington University School of Medicine. We thank Eric Ford and Hung Tran for expert technical assistance.

REFERENCES

1. Johnson, J. D., Ahmed, N. T., Luciani, D. S., Han, Z., Tran, H., Fujita, J., Misler, S., Edlund, H., and Polonsky, K. S. (2003) *J. Clin. Invest.* **111**, 1147–1160
2. Butler, A. E., Janson, J., Bonner-Weir, S., Ritzel, R., Rizza, R. A., and Butler, P. C. (2003) *Diabetes* **52**, 102–110
3. Mathis, D., Vence, L., and Benoist, C. (2001) *Nature* **414**, 792–798
4. Federici, M., Hribal, M., Perego, L., Ranalli, M., Caradonna, Z., Perego, C., Usellini, L., Nano, R., Bonini, P., Bertuzzi, F., Marlier, L. N. J. L., Davalli, A. M., Carandente, O., Pontiroli, A. E., Melino, G., Marchetti, P., Lauro, R., Sesti, G., and Folli, F. (2001) *Diabetes* **50**, 1290–1301
5. Maedler, K., Sergeev, P., Ris, F., Oberholzer, J., Joller-Jemelka, H. I., Spinas, G. A., Kaiser, N., Halban, P. A., and Donath, M. Y. (2002) *J. Clin. Invest.* **110**, 851–860
6. Efanova, I. B., Zaitsev, S. V., Zhivotovsky, B., Kohler, M., Efendic, S., Orrenius, S., and Berggren, P. O. (1998) *J. Biol. Chem.* **273**, 33501–33507
7. Moritz, W., Meier, F., Stroka, D. M., Giuliani, M., Kugelmeier, P., Nett, P. C., Lehmann, R., Candinas, D., Gassmann, M., and Weber, M. (2002) *FASEB J.* **16**, 745–747
8. Shimabukuro, M., Zhou, Y. T., Levi, M., and Unger, R. H. (1998) *Proc. Natl. Acad. Sci. U. S. A.* **95**, 2498–2502
9. Zhou, Y. P., Teng, D., Dralyuk, F., Ostrega, D., Roe, M. W., Philipson, L., and Polonsky, K. S. (1998) *J. Clin. Invest.* **101**, 1623–1632
10. Araki, E., Oyadomari, S., and Mori, M. (2003) *Intern. Med.* **42**, 7–14
11. Federici, M., Hribal, M. L., Ranalli, M., Marselli, L., Porzio, O., Lauro, D., Borboni, P., Lauro, R., Marchetti, P., Melino, G., and Sesti, G. (2001) *FASEB J.* **15**, 22–24
12. Paraskevas, S., Aikin, R., Maysinger, D., Lakey, J. R., Cavanagh, T. J., Agapitos, D., Wang, R., and Rosenberg, L. (2001) *Ann. Surg.* **233**, 124–133
13. Orrenius, S., Zhivotovsky, B., and Nicotera, P. (2003) *Nat. Rev. Mol. Cell. Biol.* **4**, 552–565
14. Scorrano, L., Oakes, S. A., Opferman, J. T., Cheng, E. H., Sorcinelli, M. D., Pozzan, T., and Korsmeyer, S. J. (2003) *Science* **300**, 135–139
15. Johnson, J. D., and Chang, J. P. (2000) *Biochem. Cell Biol.* **78**, 217–240
16. Johnson, J. D., and Misler, S. (2002) *Proc. Natl. Acad. Sci. U. S. A.* **99**, 14566–14571
17. Holz, G. G., Leech, C. A., Heller, R. S., Castonguay, M., and Habener, J. F. (1999) *J. Biol. Chem.* **274**, 14147–14156
18. Johnson, J. D., Kuang, S., Misler, S., and Polonsky, K. S. (2004) *FASEB J.* **18**, 878–880
19. Pacher, P., Thomas, A. P., and Hajnoczky, G. (2002) *Proc. Natl. Acad. Sci. U. S. A.* **99**, 2380–2385
20. Tsuboi, T., da Silva Xavier, G., Holz, G. G., Jouaville, L. S., Thomas, A. P., and Rutter, G. A. (2003) *Biochem. J.* **369**, 287–299
21. Zhao, F., Li, P., Chen, S. R., Louis, C. F., and Fruen, B. R. (2001) *J. Biol. Chem.* **276**, 13810–13816
22. Islam, M. S. (2002) *Diabetes* **51**, 1299–1309
23. Adachi, R., and Kagawa, H. (2003) *Mol. Gen. Genet.* **269**, 797–806
24. Yang, H. T., Tweedie, D., Wang, S., Guia, A., Vinogradova, T., Bogdanov, K., Allen, P. D., Stern, M. D., Lakatta, E. G., and Boheler, K. R. (2002) *Proc. Natl. Acad. Sci. U. S. A.* **99**, 9225–9230
25. Sreenan, S. K., Zhou, Y. P., Otani, K., Hansen, P. A., Currie, K. P., Pan, C. Y., Lee, J. P., Ostrega, D. M., Pugh, W., Horikawa, Y., Cox, N. J., Hanis, C. L., Burant, C. F., Fox, A. P., Bell, G. I., and Polonsky, K. S. (2001) *Diabetes* **50**, 2013–2020
26. Zhou, Y. P., Sreenan, S., Pan, C. Y., Currie, K. P., Bindokas, V. P., Horikawa, Y., Lee, J. P., Ostrega, D., Ahmed, N., Baldwin, A. C., Cox, N. J., Fox, A. P., Miller, R. J., Bell, G. I., and Polonsky, K. S. (2003) *Metabolism* **52**, 528–534
27. Hong, K., Nishiyama, M., Henley, J., Tessier-Lavigne, M., and Poo, M. M. (2000) *Nature* **403**, 93–98
28. Masumiya, H., Li, P., Zhang, L., and Chen, S. R. W. (2001) *J. Biol. Chem.* **276**, 39727–39735
29. Mitchell, K. J., Pinton, P., Varadi, A., Tacchetti, C., Ainscow, E. K., Pozzan, T., Rizzuto, R., and Rutter, G. A. (2001) *J. Cell Biol.* **155**, 41–51
30. Goll, D. E., Thompson, V. F., Li, H., Wei, W., and Cong, J. (2003) *Physiol. Rev.* **83**, 731–801
31. Drucker, D. J. (2003) *Mol. Endocrinol.* **17**, 161–171
32. Maedler, K., Spinas, G. A., Lehmann, R., Sergeev, P., Weber, M., Fontana, A., Kaiser, N., and Donath, M. Y. (2001) *Diabetes* **50**, 1683–1690
33. Srinivasan, S., Bernal-Mizrachi, E., Ohsugi, M., and Permutt, M. A. (2002) *Am. J. Physiol.* **283**, E784–E793
34. Mody, I., and MacDonald, J. F. (1995) *Trends Pharmacol. Sci.* **16**, 356–359
35. Marx, S. O., Reiken, S., Hisamatsu, Y., Jayaraman, T., Burkhoff, D., Rosemblit, N., and Marks, A. R. (2000) *Cell* **101**, 365–376
36. Fill, M., and Copello, J. A. (2002) *Physiol. Rev.* **82**, 893–922

37. Takeshima, H., Komazaki, S., Hirose, K., Nishi, M., Noda, T., and Iino, M. (1998) *EMBO J.* **17**, 3309–3316
38. Komazaki, S., Ikemoto, T., Takeshima, H., Iino, M., Endo, M., and Nakamura, H. (1998) *Cell Tissue Res.* **294**, 467–473
39. Horikawa, Y., Oda, N., Cox, N. J., Li, X., Orho-Melander, M., Hara, M., Hinokio, Y., Lindner, T. H., Mashima, H., Schwarz, P. E., del Bosque-Plata, L., Oda, Y., Yoshiuchi, I., Colilla, S., Polonsky, K. S., Wei, S., Concannon, P., Iwasaki, N., Schulze, J., Baier, L. J., Bogardus, C., Groop, L., Boerwinkle, E., Hanis, C. L., and Bell, G. I. (2000) *Nat. Genet.* **26**, 163–175
40. Podesta, M., Pitto, A., Figari, O., Bacigalupo, A., Bruzzone, S., Guida, L., Franco, L., De Flora, A., and Zocchi, E. (2003) *FASEB J.* **17**, 310–312
41. Johnson, J. D., Wong, C. J., Yunker, W. K., and Chang, J. P. (2002) *Am. J. Physiol.* **282**, C635–C645
42. Johnson, J. D., Klausen, C., Habibi, H. R., and Chang, J. P. (2002) *Am. J. Physiol.* **282**, E810–E819
43. Johnson, J. D., and Chang, J. P. (2002) *J. Neuroendocrinol.* **14**, 144–155